

# UC San Diego

## UC San Diego Electronic Theses and Dissertations

### Title

Exploring Cell Intrinsic Factors to Promote Regeneration of Injured Central Nervous System Axons

### Permalink

<https://escholarship.org/uc/item/6cj747x9>

### Author

Warsinger-Pepe, Natalie Rose

### Publication Date

2015

Peer reviewed|Thesis/dissertation

UNIVERSITY OF CALIFORNIA, SAN DIEGO

**Exploring Cell Intrinsic Factors to Promote Regeneration of Injured Central  
Nervous System Axons**

A Thesis submitted in partial satisfaction of the requirements for the degree Master of  
Science

in

Biology

by

Natalie Rose Warsinger-Pepe

Committee in charge:

Assistant Professor Daniel Gibbs, Chair  
Professor Andrew Chisholm, Co-Chair  
Associate Professor Gentry Patrick

2015



The Thesis of Natalie Rose Warsinger-Pepe is approved and it is acceptable in quality and form for publication on microfilm and electronically.

---

---

Co-Chair

---

Chair

University of California, San Diego

2015

## **DEDICATION**

To my parents for always supporting me in everything I do.

## TABLE OF CONTENTS

Signature Page.....	iii
Dedication.....	iv
Table of Contents.....	v
List of Figures.....	vi
List of Tables.....	viii
Acknowledgements.....	ix
Abstract of the Thesis.....	x
Introduction: Central Nervous System Injuries .....	1
Introduction: Unbiased Candidate Approach.....	5
Materials and Methods: Unbiased Candidate Approach.....	7
Results: Unbiased Candidate Approach .....	10
Discussion: Unbiased Candidate Approach .....	12
Future Directions: Unbiased Candidate Approach .....	14
Introduction: Hypothesis-Driven Candidate Approach.....	16
Materials and Methods: Hypothesis-Driven Candidate Approach .....	18
Results: Hypothesis-Driven Candidate Approach .....	24
Discussion: Hypothesis-Driven Candidate Approach .....	29
Future Directions: Hypothesis-Driven Candidate Approach .....	35
Figures.....	39
Tables.....	63
References.....	65

## LIST OF FIGURES

Figure 1: <i>Sequence Comparison of Non-Mutated and Mutated c-Jun</i> .....	39
Figure 2: <i>Sequence Comparison of Non-Mutated and Mutated Myc</i> .....	39
Figure 3: <i>Sequence Comparison of Non-Mutated and Mutated Smad1</i> .....	40
Figure 4: <i>Sequence Comparison of Wild Type and Constitutively Active Stat3a</i> .....	40
Figure 5: <i>Sequence Comparison of Wild Type and Dominant Negative Stat3a</i> .....	41
Figure 6: <i>Characteristic Images of Transfected DRGs on Various Substrates</i> .....	42
Figure 7: <i>Cholera Toxin B Staining of AAV2 aPKCi Treated Optic Nerves After Crush</i> .....	44
Figure 8: <i>Cholera Toxin B Staining of AAV2 shRNA PKMz Treated Optic Nerves After Crush</i> .....	45
Figure 9: <i>GFP/gCOMET Staining of Representative Optic Nerve Sections After AAV2 Injection and Crush</i> .....	46
Figure 10: <i>Nissl Staining of Representative Optic Nerve Sections to Assess Consistency of Crush</i> .....	47
Figure 11: <i>Infection of Cortical Neurons by AAV2</i> .....	48
Figure 12: <i>Regenerating CST Fibers into E14 Graft after AAV2 Treatment</i> .....	49
Figure 13: <i>Quantification of CST Axon Regeneration into E14 Grafts after AAV2 Treatments</i> .....	50
Figure 14: <i>Supplemental Figure S2 from Parker SS, et al. (PNAS 2013)</i> .....	51

Figure 15: <i>Initial Transcription Factor Screen with Individual and Combinatorial Treatments</i> .....	52
Figure 16: <i>shRNA Knockdown of PKM-<math>\zeta</math> in DRGs Compared to Transfection Control</i> .....	54
Figure 17: <i>Upregulation of <math>\alpha</math>PKC-<math>\lambda</math> in DRGs Compared to Upregulation of PKM-<math>\zeta</math></i> .....	56
Figure 18: <i>Fold Change of Total Neurite Outgrowth of shRNA Knockdown of PKM-<math>\zeta</math> and Upregulation of <math>\alpha</math>PKC-<math>\lambda</math> in DRGs</i> .....	58
Figure 19: <i>RT-qPCR of Whole Rat Retina Extract (Normalized)</i> .....	60
Figure 20: <i>Relative Levels of PKM-<math>\zeta</math> in Mouse Astrocytoma</i> .....	60
Figure 21: <i>Relative Expression levels of <math>\alpha</math>PKC-<math>\lambda</math> (PKC<math>\iota</math>) and PKM-<math>\zeta</math> (PKM) in DRGs and DRG Peripheral Axons</i> .....	61
Figure 22: <i>Percentage of E18 Hippocampal Neurons with and without Multiple Axons</i> .....	62

## LIST OF TABLES

Table 1: <i>Site-Directed Mutagenesis Primers</i> .....	63
Table 2: <i>Plasmids used in Unbiased Candidate Approach</i> .....	63
Table 3: <i>Plasmids used in Biased Candidate Approach</i> .....	64
Table 4: <i>RT-qPCR Primers</i> .....	64
Table 5: <i>AAV2 Viral Constructs</i> .....	64

## **ACKNOWLEDGEMENTS**

I would like to acknowledge Dr. Daniel Gibbs for his support and mentorship over the past two years. Opening his lab to me and mentoring me as an Undergraduate student and as a Masters student has been fundamental to my development as a scientist.

I would also like to acknowledge members of the Tuszynski Lab for their assistance, advice, support, and friendship. I would particularly like to acknowledge Mark Tuszynski for support, as well as Teresa Grider, Richard Lie, An Hoang, and Janet Weber for their assistance throughout my thesis. I would also like to thank Lori Graham, Eileen Boehle, and Sarah Im for all of their animal care. I would like to specially acknowledge Jennifer Dulin for performing the cortical injections and spinal cord surgeries and for playing an essential role in the completion of the spinal cord experiment. I would also like to thank anyone in the Tuszynski lab who took time to provide me with advice throughout my thesis.

Additionally, I would like to acknowledge our collaborator Sourav Ghosh and his lab at Yale for providing me with materials as well as guidance for my thesis. I would also like to thank Geoffrey Weiner from the Goldberg lab at UCSD for teaching me the optic nerve crush experimental technique.

Last but not least, I would like to thank my parents, my boyfriend, and my friends for their undying love and support. This thesis would not have been possible without you.

## **ABSTRACT OF THE THESIS**

### **Exploring Cell Intrinsic Factors to Promote Regeneration of Injured Central Nervous System Axons**

by

Natalie Rose Warsinger-Pepe

Master of Science in Biology

University of California, San Diego, 2015

Assistant Professor Daniel Gibbs, Chair

Professor Andrew Chisholm, Co-Chair

The identification of cell intrinsic factors that enhance the regeneration of central nervous system (CNS) axons is of particular interest for axon growth and functional recovery following traumatic injury to the nervous system. We have taken both an unbiased and hypothesis-driven approach to identify candidate factors that have the potential to enhance the regenerative capacity of injured CNS neurons. Candidates identified by both approaches were analyzed using *in vitro* and *in vivo* models to assess their potential in promoting growth of injured axons.

In the unbiased approach, multiple datasets derived from whole genome transcriptional profiling of regenerating dorsal root ganglion (DRGs) cells were used to identify a sub-set of transcription factors predicted to be master regulators of regeneration. These candidates were tested for their regenerative potential *in vitro* in DRGs utilizing lentiviral gene transfer.

Using a hypothesis-driven approach, we selected candidate factors based on a known role in axon establishment and growth during development. In this study, we identify a novel role for protein kinase M zeta (PKM- $\zeta$ ) and atypical protein kinase C iota/lambda (aPKC- $\lambda$ ). These were recently shown to regulate axon specification in developing CNS neurons. Our results suggest that PKM- $\zeta$  acts as a negative regulator and aPKC- $\lambda$  functions as a positive regulator of neurite outgrowth in adult DRGs. Complementary *in vivo* experiments in axon regeneration after optic nerve and dorsal column injury reveal inconclusive data in regards to the role of PKM- $\zeta$  and aPKC- $\lambda$  in axon regeneration.

## **Introduction: Central Nervous System Injuries**

Central nervous system (CNS) injuries range in severity but ultimately result in dramatic decreases in quality of life and health. Peripheral nervous system (PNS) injuries can result in full recovery of peripheral nerve connections. Axon regeneration does occur in injuries of the PNS but not of the CNS. PNS axon regeneration is aided by the presence of Schwann cells, phagocytes, and macrophages that help clear the lesion site of inhibitory debris as well as secrete growth-promoting neurotrophins. In the CNS, Schwann cells and phagocytes are not present. In fact, inhibitory factors remain in the lesion site, including axonal debris, myelin-associated inhibitors, astrocytes, oligodendrocytes and microglia, contributing to the inability of the CNS to regenerate after injury.

This lack of regeneration following injury of CNS axons results in permanent loss of innervations into target regions and subsequently significant functional impairments. For example, traumatic injury to the central axonal tracts of the spinal cord can result in permanent loss of motor and sensory function below the injury, with a wide range of severities [1]. Optic nerve injuries and degenerative disorders also normally result in loss of innervations into target regions and ultimately loss of function. Traumatic brain injury (TBI) and stroke also can lead to damage and death of CNS neurons that result in functional detriment. Proper treatment for these CNS injuries remains minimal and the financial burden of these injuries remains enormous. According to the National Spinal Cord Injury Statistical Center (NSCISC) there are approximately 12,500 new cases of spinal cord injury each year in the United States and specifically in 2014, there were approximately 276,000 persons alive in the

United States with a spinal cord injury [2]. The average yearly health care and living expenses for individuals with paraplegia spinal cord injuries, as reported in November 2013, was \$510,883 for the first year after injury and \$67,677 each subsequent year [2]. The average cost due to loss in wages, fringe benefits, and productivity averaged at \$70,849 yearly, as reported in November 2013[2].

The optic nerve is a central nervous system white matter tract, comprised of axons only from the retinal ganglion cells within the retina that undergoes degeneration after injury or as a result of glaucoma. Degeneration of the optic nerve ultimately results in loss of vision. Anyone can develop glaucoma, but typically individuals over 60 years of age have a higher risk of developing the degenerative disorder [3]. According to the National Eye Institute, in 2010, 1.9% of all people in the United States were affected by glaucoma [4]. Additionally, in a survey between January 2000 and December 2010, 798 active members of the U.S. Armed Forces experienced optic or cranial nerve injuries [5].

There are three main strategies to promote functional recovery of injured CNS axons. CNS axons are thought not to regenerate due to external inhibition from the environment, lack of neurotrophic support, and lack of activation of intrinsic growth pathways. External inhibition in the CNS compared to the PNS environment has been shown through promotion of CNS axon regeneration through PNS grafts within both the optic nerve and spinal cord [6] [7]. Factors in the environment of the CNS also inhibit regeneration of CNS axons, including chondroitin sulfate proteoglycans (CSPGs) and myelin-associated inhibitors (MAIs) like Nogo, myelin-associated glycoprotein (MAG), and oligodendrocyte myelin glycoprotein (OMgp) [8] [9]. A glial scar also forms in CNS injuries. This also inhibits functional regeneration beyond the

scar by acting as a physical barrier that prevents growth [10]. CNS neurons are also thought to lack intrinsic growth pathways that allow PNS neurons to regenerate and instead, either express molecules that repulse regeneration or lack receptors to allow for positive responses to guidance cues [11] [12] [13] [14]. PNS neurons are also exposed to neurotrophic factors like NGF, BDNF, GDNF and CNTF, secreted by Schwann cells that promote growth after injury unlike CNS neurons which do not come into contact with Schwann cells [15] [16] [17] [18].

Our strategy for restoring CNS injuries involves finding an intrinsic mechanism that, when perturbed, will promote axon regeneration through the inhibitory milieu of the injury site [1]. Axon regeneration has been defined as novel growth arising from the injured end of a transected axon which extends beyond the lesion site to form connections with the normal target, restoring proper function [1]. Recent work from the Tuszynski lab and others showed that neural progenitor cells (NPCs), when grafted into an adult spinal cord injury site, differentiated into neurons that extended axons over “remarkable distances” [19]. They concluded that intrinsic properties of early stage neurons can overcome the inhibitory milieu of the injury site in spinal cord injuries to make new synaptic connections that improve function [19]. The grafted NPCs also allow for host axons to regenerate and innervate the graft [19]. Additional studies in optic nerve crush models have revealed that genetic manipulation of the retinal ganglion cells can promote axon regeneration immediately following optic nerve injury, particularly with perturbation of the pTEN/mTOR pathway [20]. Using vector-based gene therapy to express a candidate gene along with a fluorescent reporter will ideally enhance visibility as well as regeneration of injured CNS axons within both the optic nerve and in the spinal cord *in vivo* [21]. We hope to find intrinsic

factors that can promote extensive regeneration in the optic nerve alone and in the spinal cord after NPC graft to elucidate therapeutic genetic targets for central nervous system injuries, particularly optic nerve and spinal cord injuries.

## **Introduction: Unbiased Candidate Approach**

Differentiated cells can be reverted back to a pluripotent cell type upon nuclear transfer of embryonic stem cell nuclei into somatic cells, revealing the potential of state-dependent transcription factors in defining cell phenotype [22]. This idea was further validated upon discover of the Yamanaka factors, four transcription factors that, when introduced into adult fibroblasts, will induce pluripotency and push those cells back to an embryonic stem (ES) cell type [23]. Transcription factors have a broad influence on cell fate as they have many downstream effectors. This makes transcription factors multi-potent targets that can promote extensive changes in gene expression within quiescent cell types, including adult CNS neurons, resulting in broad changes in cell characteristics and metabolic activity.

Transcriptomic data from regenerating PNS neurons, specifically dorsal root ganglion cells (DRGs), has been compiled by various research groups within the spinal cord injury field with the attempt to find transcription factors that, when differentially regulated in CNS neurons, will promote extensive axon growth and regeneration after injury. A list was compiled from RNAseq and microarray analysis comparing conditioned to non-conditioned DRGs to find transcription factors at hubs of gene regulation that play a role in PNS regeneration. Ingenuity analysis of the datasets resulted in the following transcription factor list: activating transcription factor 3 (ATF3), c-Jun, growth arrest and DNA-damage inducible gamma (GADD45G), Smad1, early growth response 1 (EGR1), Myc, nuclear factor 1 (NF1), zinc finger protein 367 (ZFP367), SRY-box transcription factor (Sox11), CCAAT/enhancer binding protein delta (CEBPD), signal transducer and activator of transcription 3 (Stat-3a), and p53. Some of these transcription factors have already been found to

influence peripheral nerve regeneration or neurite outgrowth, including ATF3, c-Jun, EGR1, Sox11, Stat3a, and p53 [24] [25] [26] [27] [28] [29]. Others have been found to play a role in neural development (GADD45G and Smad1), pluripotency (Myc), chromatin remodeling (NFi-1), and anti-apoptosis (CEBPD), all characteristics that, when manipulated, are hypothesized to have the potential to increase growth or regeneration of quiescent, adult neurons [30] [31] [32] [33] [34].

Post-translational modifications of transcription factors can additionally alter cellular activity drastically. Of this list of twelve transcription factors, Myc, c-Jun, Stat3a, and Smad1 were identified through bioinformatic analysis as having post-translational phosphorylation modifications that make these transcription factors constitutively active. Making these modifications is hypothesized to promote constant activity of these transcription factors and thus promote neurite outgrowth and axon regeneration to a greater extent than the non-mutated transcription factors.

Similar to Yamanaka and Takahashi, we took these twelve candidate transcription factors (including mutated and non-mutated variants) with the goal to perform a subtraction screen to find the few, key transcription factors that, when up-regulated in combination in adult DRGs, would promote the most neurite outgrowth on myelin [23]. Myelin, and its associated inhibitors, like Nogo, MAG and OMgp have been shown to inhibit axon growth after CNS injury and is used in these studies to represent an inhibitory external environment, *in vitro* [9] [35]. We hypothesize that these “master regulators” that promote the most neurite outgrowth in DRGs *in vitro* when cultured on myelin, will promote the most axon regeneration *in vivo* in CNS injuries including optic nerve trauma and spinal cord injuries.

## **Materials and Methods: Unbiased Candidate Approach**

### *Plasmid Production and Site-Directed Mutagenesis*

The plasmids listed in Table 2 were either previously cloned or personally cloned using In-Fusion cloning (ClonTech, 638912). Three constructs, highlighted in yellow, were modified through site-directed mutagenesis to create constitutively active forms of the wild type transcription factor. The primers that were designed for site-directed mutagenesis are listed in Table 1. For each reaction, the original plasmids were fully amplified using the site-directed mutagenesis primers. CloneAmp HiFi Premix (Clontech, 639298) was used to amplify the plasmid using PCR along with 50ng of template plasmid, and 125ng of each primer. A PCR cycle ran on a BIO-RAD MJ Mini Personal Thermal Cycle conditions were as follows: Step 1 at 98°C for 30 seconds, Step 2 at 55°C for 15 seconds, Step 3 at 68°C for 3.5 minutes, all repeated for a total of 12 cycles. After PCR amplification, the PCR product was incubated on ice for 2 minutes then digested with 1µl DpnI (NEB, R0176S), added directly to the amplification reaction. This was then mixed and incubated at 37°C for 1 hour. The newly mutated plasmids were then transformed into NEB5α competent cells (NEB, C2987H), with 2µl of amplified DNA to 50µl competent cells. The transformed cells were plated on LB-Agar plates and incubated at 37°C overnight. Colonies were picked the following day, DNA was isolated using a Qiaprep Spin Miniprep Kit (Qiagen, 27106) and the sequence was verified using services provided by Eton Sequencing.

### *Lentivirus Production*

Lentivirus was produced from each plasmid listed in Table 2 (excluding pRRL-CMV-Comet-Stat3a-F (DN)) following the protocol as detailed by Tiscornia et al [36]. The MOI was determined through cell counts of infected HEK293T cells, counting the cells expressing the green fluorescent reporter protein, GFP/gCOMET.

#### *DRG Extraction, Transduction, and Culture*

Adult rats (Fischer 344) were anesthetized with an overdose amount of xylazine/acepromazine/ketamine and sacrificed. DRGs were isolated, dissociated and cultured using optimized conditions as described by McCall et al [37]. DRGs were either plated at 50,000 cells per well onto 24-well tissue culture treated plates or 2,000 DRGs per well onto a 48-well plate. Plates were pre-coated with either of the following combination of substrates: A) poly-D-lysine hydrobromide at 20 µg/ml in diH<sub>2</sub>O (PDL) (Sigma-Aldrich, P6407), B) PDL and laminin at 0.5 µg/ml in dPBS (PDL/LAM) (Sigma-Aldrich, L2020-1MG), or C) PDL/LAM and extracted rat myelin at 10-25 µg/ml in dPBS, (PDL/LAM/MYL). DRGs were infected with lentivirus at an MOI of ~10 per viral construct 4-6 hours post plating. Media was changed the following day and the cells were fixed after 3 DIV.

#### *DRG Immunocytochemistry*

After 2 DIV, DRG cultures were fixed with 4% Formaldehyde in PBS for 20 minutes at room temperature, washed three times with PBS, permeabilized with PBS plus 0.025% Triton X-100 for 20 minutes at room temperature, washed and then blocked in PBS and 10% goat serum for one hour. DRGs were incubated overnight at 4°C with the following primary antibodies: Mouse anti-βIII-Tubulin (Promega, 1:2000)

and Rabbit anti-GFP (Invitrogen, 1:1500). Secondary antibodies include Alexa Fluor 594 anti-mouse, Alexa Fluor 488 anti-rabbit (Invitrogen, 1:1000). Nuclei were counterstained with DAPI (Invitrogen, 1:1000). Cells were incubated with secondary antibodies for one hour at room temperature, washed and stored at 4°C in PBS. Plates were imaged using the ImageXpress automated microscopy system and MetaXpress software was used to quantify neurite outgrowth data (Molecular Devices, Sunnyvale, CA). Three to six replicated wells were analyzed for each plating condition and experimental treatment.

## **Results: Unbiased Candidate Approach**

### *Mutated Transcription Factors through Site-Directed Mutagenesis*

Through bioinformatics and literature review, phosphorylation sites for c-Jun, Myc, and Smad1 were identified that have been experimentally verified to promote activity once phosphorylated. The sequences of the un-mutated transcription factors were analyzed and primers for site-directed mutagenesis were designed to mutate the nucleotide sequence, taking tRNA prevalence in rat into account, to ultimately change the amino acid sequence and generate constitutively active transcription factors. As seen in the sequence chromatograms in Figures 1-3, c-Jun, Myc, and Smad1 were successfully mutated through site-directed mutagenesis using primers listed in Table 1. c-Jun was mutated at S63D and S73D (Figure 1), Myc was mutated at T58A (Figure 2), and Smad1 was mutated at S465D, S466D, and S468D (Figure 3). Stat3a had been previously mutated to a constitutively active form as well as a dominant negative form and these were confirmed by sequence analysis (Figure 4, Figure 5). Analysis of function compared to un-mutated and dominant-negative forms of the transcription factors in DRGs is currently underway.

### *Transcription Factor Screen*

As seen in Figure 15, significant neurite outgrowth, determined by relative neurite area was assessed, and compared to an untreated EGFP only control condition. Unpaired t-tests were performed resulting in significant results for DRGs treated with Sox11, Stat3a-C, c-Jun-CA (constitutively active), Smad1-CA, and for the pooled transcription factors (Figure 15). These p-values are as follows: Sox11 ( $p = 0.00787$ ), Stat3a-C ( $p = 0.00290$ ), c-Jun ( $p = 0.0218$ ), Smad1 (mut) ( $p = 0.0464$ ) and

pooled transcription factors ( $p = 0.0092$ ). All processing and analysis were blinded, detracting from any bias during analysis. Since the neurite area was also normalized to cell body area, the size distribution of DRG cell bodies across a sample of the treatments were analyzed and were found to be similar (data not shown).

This data identifies the transcription factors Sox11, Stat3a-C, c-Jun-mut (c-Jun-CA), Smad1-mut (Smad1-CA), and the pooled treatment of all 13 transcription factors (with the mutated, constitutively active, transcription factors only) significantly enhanced neurite outgrowth of treated adult DRGs through a potentially inhibitory milieu. However, the DRGs were initially plated at 2500 DRGs per well in 48-well plates and were fixed after 3 DIV resulting in extremely overgrown cultures on laminin, a growth-permissive substrate, and less overgrown cultures on myelin. The cultures grown on laminin were not analyzed due to this caveat.

As a result of these caveats, this data remains preliminary but suggests a potential positive influence of Sox11, Stat3a-C, c-Jun-CA, Smad1-CA, and the pooled transcription factors combined (with mutated factors) on neurite growth.

## **Discussion: Unbiased Candidate Approach**

### *Transcription Factor Screen*

These twelve transcription factors were identified through bioinformatic analysis of many genomic screens (microarray and RNA-seq) of regenerating DRGs as the top candidate network hubs. These twelve transcription factors represent master regulators of DRG peripheral regeneration. Four transcription factors were identified to have post-translational modifications particularly phosphorylation sites that cause these transcription factors to be constitutively active. These transcription factors were successfully mutated as discussed previously and analysis of functional relevance in DRGs compared to the un-mutated forms of the transcription factors is underway.

After the initial transcription factor screen, Sox11, Stat3a-C, c-Jun-CA, Smad1-CA and the pooled transcription factors combined (with mutated factors) were found to significantly increase neurite growth on myelin, a potent growth-inhibiting substrate. Also, whilst not all were significant, all chosen transcription factors showed enhanced growth compared to control. These phenomena could be a result of toxicity of the lentivirus expressing EGFP, or that all of the transcription factors have a positive effect, which is supported by the combined transcription factor treatment. This result also accents the power of combining unbiased genomic analysis with cell-based screening to identify and functionally validate candidate genes and pathways important for regeneration. Performing a subtraction screen of these transcription factors will allow us to accomplish our ultimate goal to identify a minimal cohort of transcription factors that drive robust regeneration. This resultant list of transcription

factors will be key targets for drug intervention to therapeutically enhance neural regeneration in clinical cases of CNS and PNS nerve injury.

## **Future Directions: Unbiased Candidate Approach**

### *Neurite Outgrowth of Mutated Transcription Factors*

To test functional differences between the mutated and un-mutated transcription factors, both the mutated and un-mutated transcription factors will be tested *in vitro* in adult DRGs to assess for any increase or decrease in neurite outgrowth on both growth-permissive and growth-inhibitory substrates.

### *Transcription Factor Subtraction Screen*

To find the key master regulators of regeneration from these 17 transcription factors (including the mutated CA versions and dominant negative Stat3a), an initial screen of neurite outgrowth will be performed to repeat the original assay. Then the most effective single factors (mutated or non-mutated) will be tested in a subtraction screen. Initially, the first round of the subtraction screen with the twelve transcription factors pooled together (including most effective mutated or un-mutated transcription factors) will be pooled to infect cultured DRGs to assess for neurite outgrowth. Then, the subtraction screen will be performed, where one factor is removed at a time at subsequent steps in the screen, similar to the seminal subtraction screen performed by Takahashi and Yamanaka that successfully identified four factors minimally required to induce pluripotency (iPSC) in adult somatic cells [23]. After each subsequent assay, one transcription factor will be removed from each condition to assess any differences in neurite outgrowth. This subtraction approach will identify which of these factors promote the most neurite outgrowth in adult DRGs. Candidates found to enhance neurite outgrowth to a significant degree will then be subject to additional rounds of subtraction screening until a minimal group of factors (ideally less

than 6) are identified that are sufficient, in combination, to promote robust neurite outgrowth on myelin compared to all other treatments.

In order to be confident that the transcription factors have enough time to be expressed, influence downstream effectors, while also not allowing the cultures to become overgrown, a re-plating technique will be applied to all DRG cultures. Re-plating the DRGs after 2 DIV will also allow for neurite outgrowth analysis to not be influenced by differences in neurite initiation pre-infection. DRGs will be plated and infected using lentiviral gene transfer, re-plated after 3-4 DIV, and analyzed for neurite outgrowth between 12-24 hours post re-plating. This technique is broadly used and will allow for more accurate assessment of the influence of these transcription factors on neurite outgrowth. Analysis of neurite outgrowth will also be performed using calibrated neurite outgrowth programs after imaging using the MetaXpress system allowing for consistent, un-biased analysis of neurite outgrowth based on pixel length of each neurite extending outwards from a positively infected DRG.

## Introduction: Hypothesis-Driven Candidate Approach

To promote regeneration of injured CNS axons to the extent that will allow for functional recovery, it has generally been hypothesized that modifying the molecular state of the injured neurons to mimic either a PNS or a developmental phenotype, will promote a state of regeneration in the adult CNS [7] [19]. Mechanisms that promote growth during normal embryonic development, a period of vigorous axonal growth, are promising molecular candidates for promoting CNS regeneration. Wnt proteins are an example of factors that not only play key roles in early embryonic development of the nervous system in invertebrates as well as vertebrates, but are suggested to play a role in tissue and axon regeneration after injury [38] [39] [40].

This project examines the role of two atypical protein kinase C isoforms: protein kinase M-zeta (PKM- $\zeta$ ) and atypical protein kinase C-lambda (aPKC- $\lambda$ ) in neurite outgrowth in PNS neurons and their potential role in axon regeneration of CNS neurons. The role of PKM- $\zeta$  in learning and memory has been studied extensively, yet remains controversial and undetermined. PKM- $\zeta$  was initially thought to be both necessary and sufficient for long term potentiation [41]. This was contradicted by the finding that the pharmacological PKM- $\zeta$  inhibitors used in these studies, namely ZIP and Chelerythrine, whilst capable of inhibiting purified PKM- $\zeta$  *in vitro*, did not inhibit PKM- $\zeta$  in cultured cells or in brain slices [42] [43]. Also, *Prkcz* null mice, lacking both aPKC- $\zeta$  and its truncated and neuron-specific form, PKM- $\zeta$ , did not show any learning or memory deficits [44] [43]. Together, these reports strongly suggest that PKM- $\zeta$  does not play a central role in learning and memory.

Alternately, aPKCs have been known to play an important role in the polarization of both neurons and epithelial cells through binding of Par polarity

signaling complexes [45]. Recently, two particular aPKC isoforms were discovered to play a key role in axon specification [44]. It was elucidated that the competition of PKM- $\zeta$  and aPKC- $\lambda$  for Par3 complex binding regulates axon specification of developing embryonic day 18 (E18) hippocampal neurons [44]. Direct evidence was found indicating that the spatial segregation of Par3 bound PKM- $\zeta$  and Par3 bound aPKC- $\lambda$  complexes results in axon suppression or formation, respectively [44]. Overexpression of aPKC- $\lambda$  and shRNA knockdown of PKM- $\zeta$  results in supernumerary axon formation; overexpression of PKM- $\zeta$  results in axon suppression [44]. These results were similarly recapitulated in hippocampal neurons from *Prkcz*<sup>-/-</sup> mice (Ghosh unpublished data, Figure 22). Additionally, the PNS sensory branch of DRGs have been shown to have reduced levels of PKM- $\zeta$  compared to the CNS branch, suggesting a competitive role not only in development, but in maintaining characteristics of the PNS and the CNS [46]. Since these aPKCs regulate specification of axons in early stage neurons and appear to be differentially expressed in the PNS and CNS, we hypothesize that these atypical protein kinases may promote neurite outgrowth and axon regeneration in injured adult PNS and CNS neurons. To test this hypothesis, we tested the influence of overexpressing aPKC- $\lambda$  and knocking down PKM- $\zeta$  utilizing RNAi in three different experimental paradigms: DRG neurite outgrowth *in vitro*, RGC regeneration after optic nerve crush *in vivo*, and CST regeneration after dorsal column lesion and E14 spinal cord NPC graft *in vivo*.

## **Materials and Methods: Hypothesis-Driven Candidate Approach**

### *Plasmids*

The following plasmids were kindly provided by Dr. Sourav Ghosh (Yale University): pLeGO-T-shRNA PKM- $\zeta$ , pFLAG-3x- PKM- $\zeta$ , pFLAG-3x- aPKC- $\lambda$  and pLeGO-iT-3xFLAG- aPKC- $\lambda$ . Plasmids were purified using the 5 Prime PerfectPrep Endofree Plasmid Maxi Kit according to instructions (5 Prime) or Qiagen Maxi Kit. A plasmid expressing a scrambled shRNA was purchased from Addgene from the depositing lab of Dr. David Sabatini [47] and was cloned using infusion cloning (CloneTech) to make the following plasmid: pAAV-CAG-Comet-U6-scramble shRNA. The plasmids listed in Table 3 were cloned using infusion cloning (CloneTech) or Gibson Assembly Kit (New England Biosciences, E2611L).

### *DRG Extraction, Transfection, and Culture*

Adult rats (Fischer 344) were sacrificed and DRGs were isolated, electroporated, and cultured using optimized conditions as described by McCall et al [37]. DRGs were plated as previously described.

### *DRG Immunocytochemistry*

After 2 DIV, DRG cultures were fixed, permeabilized and blocked as previously described. The DRGs were incubated overnight at 4°C with a combination of the following primary antibodies: Mouse anti- $\beta$ III-Tubulin (Promega, 1:2000) and Rabbit anti-RFP (Abcam, 1:300) or Rabbit anti- $\beta$ III-Tubulin (Covance, 1:1000) and Mouse anti-flag (Sima-Aldrich, 1:200). Secondary antibodies include Alexa Fluor 488 anti-mouse, Alexa Fluor 594 anti-rabbit, Alexa Fluor 488 anti-rabbit, and Alexa Fluor

594 anti-mouse (Invitrogen, 1:1000). Nuclei were counterstained with DAPI (1:1000). Immunocytochemistry and analysis were performed as previously described.

#### *RT and qPCR Verification of PKM- $\zeta$ Knockdown in DRGs*

DRGs were extracted, dissociated and cultured as described earlier. DRGs were plated at either 25,000 cells/well or 50,000 cells per well in wells that were previously coated with PDL and laminin. Cells were plated immediately after dissociation. One hour post plating, cells were infected with either lentivirus encoding the shRNA against PKM- $\zeta$ , AAV2 encoding the shRNA against PKM- $\zeta$ , AAV2 overexpressing GFP/gCOMET, or were left uninfected. After 3DIV, total RNA from the DRGs was isolated using an RNeasy Mini Kit (Qiagen, 74106) and an RNase-Free DNase Set (Qiagen, 79254). cDNA was generated using PrimeScript RT Master Mix (Perfect Real Time) (ClonTech, RR036A) and qPCR was performed on a BIO-RAD myIQ Thermal Cycle using SYBER Premix Ex Taq II (Tli RNaseH Plus) (ClonTech, RR820A) and the primers listed in Table 4.

#### *Adeno-associated Virus Serotype 2 (AAV2) Production*

Adeno-associated virus, serotype 2, (AAV2) was produced by the University of Northern Carolina and the GT3 Core at the Salk Institute (Table 5).

#### *Intravitreal Injections of AAV2*

Concentrated AAV2 (2-5 $\mu$ l per eye) was injected into the vitreous of separate eyes of adult rat female Sprague-Dawley or Fisher rats using capillary injection techniques. The viruses injected are listed in Table 5. Animals were anesthetized

using ketamine/domitor and a guide incision in the sclera was made with a 27gauge needle. Some intravitreal fluid was allowed to drain prior to injection to prevent build-up of intraocular pressure. Immediately following, 2-5 $\mu$ l of AAV2 around a 10E12 titer was injected into the vitreous at a 45 degree downward angle taking care to avoid damaging the lens. All animals were treated according to UCSD and VA guidelines, and in compliance with the ARVO statement on the use of animals for ophthalmic and vision research. NIH guidelines for laboratory animal care and safety were strictly followed. Animals had free access to food and water throughout the study.

#### *RT and qPCR Verification of PKM- $\zeta$ Knockdown in RGCs*

Retinas of adult fisher rats were infected with AAV2 virus through intravitreal injections according to the protocol described previously. NIH guidelines for laboratory animal care and safety were strictly followed. Animals had free access to food and water throughout the study. After two weeks, animals were anesthetized with a lethal dose of xylazine/acepromazine/ketamine and sacrificed. The retinas were extracted and dissociated using Papain (Worthington, LK003176), resuspended in FACs buffer (1% BSA and 5mM EDTA in dPBS) and FACS was performed to select green fluorescent cells. Successfully infected, green fluorescent cells were sorted into HBSS. Total RNA from the RGCs was isolated, cDNA was produced, and qPCR was performed as previously described.

#### *Optic Nerve Crush Surgery, Zymosan Injections, CTB Tracing*

Optic nerve crush surgeries were performed on adult female Sprague-Dawley or Fisher rats two days or one week post AAV2 injection. Rats were anesthetized with

ketamine/domitor and the optic nerve crush (ONC) was performed by blunt dissection through and below the sclera, following along the orbit. The optic nerve was crushed mechanically using thin, curved surgical forceps for 10 seconds, 3mm from the orbit. In positive control animals, 7 $\mu$ l of Zymosan (Invivogen, tlr1-zyn) diluted at 10mg/ml in endonuclease-free water was injected via intravitreal injections as previously described, immediately following ONC. Three days before sacrificing the animals, the optic nerves were traced with 3 $\mu$ l of 1%Cholera Toxin B subunit in sterile water (List Biologicals #104) via intravitreal injections as previously described. NIH guidelines for laboratory animal care and safety were strictly followed. Animals had free access to food and water throughout the study.

#### *Retina and Optic Nerve Tissue Processing*

Two-three weeks post-crush, rats were anesthetized with a lethal dose of xylazine/acepromazine/ketamine and perfused with saline and 4% PFA. The heads of each animal were post-fixed in 4% PFA overnight. The retinas were post-fixed in 4% PFA for two hours post perfusion and transferred to 30% sucrose. The optic nerves were dissected after post-fixation and were placed, along with the retinas, in 30% sucrose.

#### *Retina and Optic Nerve Immunohistochemistry and Analysis*

Whole retinas and optic nerve sections, sectioned at 12 $\mu$ m on a Leica Cryostat and direct mounted onto subbed slides, were treated with 50% and 100% methanol for antigen retrieval. The tissue samples were incubated in blocking buffer and then stained with primary antibody overnight at 4°C. The retinas were stained

with Rabbit anti-GFP (Evrogen, 1:1500) and Mouse anti-Brn3a (Millipore, 1:50). The optic nerve sections were stained with Mouse anti-pan Neurofilament (Covance, 1:750) or Mouse anti-GAP-43 (Millipore, 1:500), Goat anti-CTB (List Biologicals, 1:2500), and Rabbit anti-GFP (Invitrogen, 1:1500). The tissue samples were washed and then stained with secondary antibody and mounted in Mowiol. Nissl staining was also performed on some optic nerve sections. The retinas were stained with AlexaFluor 488 anti-rabbit (Invitrogen, 1:500), Alexa Fluor 647 anti-mouse (Invitrogen, 1:500), and counterstained with DAPI (1:1000). The optic nerve sections were stained with AlexaFluor 488 anti-rabbit (Invitrogen, 1:250), AlexaFluor 594 anti-goat (Invitrogen, 1:250), AlexaFluor 647 anti-mouse (Invitrogen, 1:250), and DAPI (1:1000). All tissue samples were imaged on the all-in-one fluorescence microscope BZ-X700 (Keyence).

#### *Cortical AAV2 Injections*

AAV2 viruses listed in Table 5 were separately injected into the cortex of anesthetized adult Fisher rats at  $2.4 \times 10^{12}$  IU/ml into 4 sites per hemisphere into bilateral motor cortices, 0.5 $\mu$ l per site as previously described [19]. NIH guidelines for laboratory animal care and safety were strictly followed. Animals had free access to food and water throughout the study.

#### *C4 Dorsal Column Lesion and E14 Spinal Cord Grafting*

One week post AAV2 injection, rats received a C4 dorsal column lesion immediately followed by grafting of wild-type E14 spinal cord neural stem cells (NSCs).  $1 \times 10^6$  cells were embedded within a fibrin matrix with full growth factor

cocktail and were grafted into the lesion sites as previously described [19]. NIH guidelines for laboratory animal care and safety were strictly followed. Animals had free access to food and water throughout the study.

#### *Spinal Cord and Brain Immunohistochemistry and Analysis*

Four weeks post spinal cord injury and engraftment, rats were anesthetized, sacrificed, and perfused as described above. Saggital sections of the spinal cords (30 $\mu$ m) encompassing the lesion and graft site were stained with rabbit anti-Calretinin (1:1000), mouse anti-NeuN (1:500), and chicken anti-GFP (Abcam, 1:10,000) primary antibodies. GFP signal was twice amplified using tyramide signal amplification (TSA) (Life Technologies, T20931). The sections were stained with goat anti-rabbit AlexaFluor 647 (Invitrogen, 1:1000), goat anti-mouse AlexaFluor 555 (Invitrogen, 1:1000), and streptavidin conjugated AlexaFluor 488 (Invitrogen, 1:1000) secondary antibodies. Sections were also counterstained with DAPI (1:1000). Coronal brain slices (30 $\mu$ m) encompassing the injection sites were stained with rabbit anti-phospho-S6 (Cell Signaling, 1:250), mouse anti-NeuN (1:500), and chicken anti-GFP (Abcam, 1:3000) primary antibodies. Phospho-S6 signal was amplified once using TSA as mentioned previously. These sections were stained with donkey anti-chicken AlexaFluor 488 (Invitrogen, 1:1000), donkey anti-mouse AlexaFluor 568 (Invitrogen, 1:1000), streptavidin conjugated AlexaFluor 568 (Invitrogen, 1:1000) secondary antibodies. Sections were mounted in Mowiol, dried overnight, and imaged on the all-in-one fluorescence microscope BZ-X700 (Keyence). Saggital spinal cord sections were analyzed for axon growth into the graft using ImageJ.

## **Results: Hypothesis-Driven Candidate Approach**

### *DRG Neurite Outgrowth Assay*

Adult rat DRGs overexpressing PKM- $\zeta$ , aPKC- $\lambda$  or an shRNA construct targeting PKM- $\zeta$  were analyzed 2 days post transfection for neurite outgrowth, total branching, number of processes, and maximum processes length on poly-D-lysine (PDL), a growth-neutral substrate, on laminin (PDL/LAM) a growth-promoting substrate, and on myelin (PDL/LAM/MYL) a growth-inhibiting substrate. DRGs overexpressing PKM- $\zeta$  and DRGs overexpressing aPKC- $\lambda$  were compared for analysis. DRGs expressing an shRNA targeting PKM- $\zeta$  and DRGs overexpressing an RFP control were compared for analysis.

Treatment with shRNA against PKM- $\zeta$  led to significant increases in total neurite outgrowth, total branching, and maximum process length on laminin (PDL/LAM) and myelin (PDL/LAM/MYL) relative to control DRGs expressing RFP only (Figure 16). A significant increase in the number of processes on all substrates was also seen (Figure 16).

Overexpression of aPKC- $\lambda$  also led to significant increases in total neurite outgrowth total branching, and maximum process length on laminin (PDL/LAM) and on myelin (PDL/LAM/MYL) relative to overexpression of PKM- $\zeta$  (Figure 17). Overexpression of aPKC- $\lambda$  also resulted in significant increases in number of processes on myelin (PDL/LAM/MYL) compared to overexpression of PKM- $\zeta$  (Figure 17). Experiments comparing overexpression of these two constructs to control RFP expressing cells were not conclusive due to unequal fluorescent intensity between Flag staining and RFP fluorescence.

Together, these findings indicate that treatment with shRNA against PKM- $\zeta$ , or alternatively overexpression of aPKC- $\lambda$  promotes extensive neurite outgrowth in a growth-permissive and growth-inhibitory environment and both conditions can overcome myelin-mediated inhibition.

#### *Confirmation of Knockdown of PKM- $\zeta$ by shRNA*

Experiments performed to confirm knockdown of PKM- $\zeta$  by shRNA through RT-qPCR analysis were unsuccessful. DRGs were cultured and infected with either lentivirus or AAV2 expressing the shRNA against PKM- $\zeta$  and RT-qPCR was performed to check for levels of GAPDH, aPKC- $\lambda$ , aPKC- $\zeta$ , and PKM- $\zeta$  compared to AAV2 control as well as to untreated DRGs. Experiments were also performed to confirm knockdown of PKM- $\zeta$  by shRNA through RT-qPCR analysis in infected RGCs *in vivo*. Retinas were dissociated and sorted through FACS and RT-qPCR was performed. These experiments were inconclusive due to low levels of GAPDH.

#### *Regeneration after Optic Nerve Crush*

The optic nerve consists of purely white matter axonal tracts from retinal ganglion cells, making it a good model for CNS regeneration after injury. The optic nerve crush model is an extensively used model and can show robust regeneration upon genetic manipulation [20] [48] [49]. Our qualitative results demonstrate that our positive control for axonal regeneration, Zymosan and AAV2-GFP/gCOMET treatment of RGCs immediately after optic nerve crush, was able to promote moderate axon regeneration beyond the crush site as compared to control retinas only infected with AAV2-GFP/gCOMET (Figure 7, Figure 8). In agreement with published reports, one injection of Zymosan would be predicted to only promote

moderate levels of axon regeneration as compared to multiple injections of Zymosan, confirming the validity of the experimental model [50]. The extent of optic nerve crush was also qualitatively assessed and revealed no significant differences in crush size or severity (Figure 10).

Qualitative analysis of CTB axonal tracing following optic nerve crush from either aPKC- $\lambda$  treated or shRNA-PKM- $\zeta$  treated optic nerves revealed very insignificant growth, if any beyond the crush site as compared to Zymosan treated RGCs (Figure 7, Figure 8). These results were visually similar to the optic nerves after RGC infection with AAV2-GFP/gCOMET (Figure 7, Figure 8). These qualitative results reveal a lack of significant influence on regeneration of RGC axons by both treatments: aPKC- $\lambda$  treated and shRNA against PKM- $\zeta$  treated RGCs.

Qualitative GFP/gCOMET expression is minimal in shRNA-PKM- $\zeta$  treated optic nerves compared to both positive and negative controls (Figure 9). GFP/gCOMET expression is also completely lacking in aPKC- $\lambda$  treated optic axonal labeling which may possibly be due to insufficient infection of RGCs by the viruses. Also, both treatments may lack neuroprotective mechanisms to aid in RGC survival. Alternatively, the modulation of the relative levels of these aPKC isoforms could stimulate RGC cell death. This may be as a result of increased downstream NF $\kappa$ B activation by aPKC- $\lambda$  and thus a potential increase in NF $\kappa$ B induced apoptosis [51] [52]. Future treatments will be administered with Zymosan injections or along with lens injury to promote neuroprotection [50] [53]. Either of these additions will allow for assessment of regenerative potential instead of the ability to both protect RGCs and regenerate their injured axons.

### *Regeneration of CST Axons after C4 Dorsal Column Lesion and E14 Graft*

The corticospinal tract (CST) has been shown to regenerate extensively into embryonic day 14 (E14) spinal cord neural stem cell grafts after injury [19]. Layer 5b cortical neurons extend their axons into the spinal cord and are essential for fine motor control. Upon infection of layer 5b cortical neurons, axons leading from the soma to the spinal cord become labeled with GFP/gCOMET, the fluorescent reporter gene. As seen in Figure 11, the viruses resulted in variable infection of and/or variable GFP/gCOMET expression in the cortical neurons. Qualitatively, fewer cells appear to be expressing GFP/gCOMET in the shRNA-PKM- $\zeta$  treated cortical neurons compared to GFP/gCOMET control treated cortical neurons. Additionally, no cells appear to be expressing GFP/gCOMET in the aPKC- $\lambda$  treated cortical neurons. As seen in Figure 12, aPKC- $\lambda$  treated CST fibers do not show any GFP/gCOMET expression, making the effect of this treatment remain inconclusive. CST fibers treated with either GFP/gCOMET control or shRNA-PKM- $\zeta$  show growth into the graft (Figure 12). Quantification of the percentage of the graft area consisting of GFP/gCOMET labeled CST axons of the GFP/gCOMET control and of shRNA against PKM- $\zeta$  treated CST shows a decrease through the graft for the GFP/gCOMET control treatment and significantly lower values through the graft for the shRNA against PKM- $\zeta$  treated CST (Figure 13). This reveals potentially negative effect of the shRNA against PKM- $\zeta$  treatment on regeneration of the CST axons after injury, compared to GFP/gCOMET control. However, quantification of the GFP positive fibers into the graft was dependent on GFP/gCOMET expression. Since both the intensity of GFP/gCOMET expression, and the density of GFP/gCOMET labeled axons in the graft was lower in the shRNA against PKM- $\zeta$  treated CST, this resulted in

an underrepresentation of the infected axons growing into the graft compared to control GFP/gCOMET axons. Quantification normalizing GFP/gCOMET expression and GFP/gCOMET labeled axon density in the graft to the expression and labeling density in the CST main tract rostral to the lesion will be performed within each treatment to account for this caveat in axon quantification.

## Discussion: Hypothesis-Driven Candidate Approach

### *DRG Neurite Outgrowth Assay*

Through our *in vitro* DRG analysis, we showed that treatment with shRNA against PKM- $\zeta$  potentially increases total neurite outgrowth, total cell branching, number of processes, and maximum process length in the presence of myelin relative to a transfection control (Figure 16). We also showed that the overexpression of aPKC- $\lambda$  increases total neurite outgrowth, total cell branching, number of processes, and maximum process length in the presence of myelin relative to the overexpression of PKM- $\zeta$  (Figure 17). These findings confirmed our initial hypothesis and demonstrated that modulating the relative expression levels of aPKC isoforms significantly enhanced the regenerative capability of adult neurons. Adult DRG neurons demonstrated enhanced axonal growth in an already stimulatory environment as well as the ability to overcome a strongly inhibitory external environment. These *in vitro* results from DRG neurons led us to test the potential of knocking down PKM- $\zeta$  or overexpressing aPKC- $\lambda$  to stimulate axon regeneration *in vivo* in CNS injury models where myelin is a prevalent source of inhibition and where the intrinsic growth state after injury is not sufficient to initiate regeneration. These findings also led us to believe that knocking down PKM- $\zeta$  and overexpressing aPKC- $\lambda$  in combination could promote further neurite outgrowth *in vitro* and promote axon growth *in vivo* and will be tested in future experiments.

The overexpression constructs of both PKM- $\zeta$  and aPKC- $\lambda$  in DRGs could not be compared directly to the RFP transfection control because the PKM- $\zeta$  and aPKC- $\lambda$  expressing plasmids do not contain an RFP reporter gene. Instead, the constructs contain a triple FLAG sequence conjugated to the protein of interest, so

immunocytochemistry was performed against the FLAG sequence and amplified with an AlexaFluor secondary antibody conjugated with 594nm fluorophore. This fluorescence was weaker and differentially distributed compared to the native fluorescence of the RFP or tdTomato from the control or shRNA-PKM- $\zeta$  treated cells, respectively. Automated comparison of FLAG labeled cells to red fluorescent protein labeled cells led to artifactual differences in neurite measurements between the two groups, although measurements within the two groups were internally consistent. This caveat is somewhat of a concern since we do not have a common baseline to use as a control for all of our treatments. However, since we see a significant difference when comparing overexpression of PKM- $\zeta$  and aPKC- $\lambda$ , we are inclined to believe that overexpressing aPKC- $\lambda$  compared to overexpressing PKM- $\zeta$  does result in significant differences in neurite outgrowth. These constructs have been re-cloned into consistent plasmid backbones with the same GFP/gCOMET reporter to be tested in future repeats of this experiment to overcome this problem in analysis.

Another area of concern lies within the discrepancy between the outgrowth numbers of the knockdown experiment compared to the overexpression experiment. The overexpression experiment resulted in a ten-fold lower outgrowth number than the first knockdown experiment. However, it is likely that this 10-fold difference is an artifact due to problems with classification described above, as preliminary manual measurements of neurite growth of DRGs and fold change measurements from both treatments indicate values and changes well within the same order of magnitude (Figures 16-18). DRG growth also varies across different experiments as a result of preparation and plating variability. Based on this data, our conclusions on the effects of aPKC- $\lambda$  on neurite outgrowth and axon regeneration still remain preliminary and

duplicate experiments are underway to further test its influence on neurite outgrowth in DRGs, but we hypothesize that we will see similar effects on neurite outgrowth in future *in vitro* experiments with DRGs.

#### *Confirmation of Knockdown of PKM- $\zeta$ by shRNA*

Whereas experiments to confirm knockdown of PKM- $\zeta$  by shRNA in DRGs and FACS sorted RGCs were unsuccessful, some knowledge can be gleaned from the RT-qPCR experiments. RT-qPCR against whole rat retina extract confirms that PKM- $\zeta$  (as well as other aPKC isoforms) is expressed in the retina, suggesting that RGCs should also express PKM- $\zeta$  (Figure 19).

Although we were unable to directly confirm knockdown of PKM- $\zeta$  by shRNA in DRGs, RGCs, or adult CST neurons, unpublished RT-qPCR data from our collaborators confirm that the shRNA construct against PKM- $\zeta$  does successfully knockdown PKM- $\zeta$  in a mouse astrocytoma cell line that overexpresses PKM- $\zeta$  (Figure 20). We are in the process of expanding our DRG cell cultures to provide larger amounts of starting material to confirm efficient and specific knockdown of PKM- $\zeta$ . The specificity of similar siRNA sequences against PKM- $\zeta$  compared to a scrambled shRNA in rat hippocampal neurons, however, showed successfully knockdown of PKM- $\zeta$  at the mRNA and protein levels while also having minimal influence on aPKC- $\lambda$  and aPKC- $\zeta$  at the protein level, we believe that we will see similar results in rat with our shRNA construct (Figure 14) [44].

#### *Regeneration after Optic Nerve Crush*

Qualitatively, treatment of RGCs with AAV2 expressing aPKC- $\lambda$  or expressing shRNA against PKM- $\zeta$  do not appear to promote regeneration of injured axons beyond the crush site compared to Zymosan+AAV2-GFP/gCOMET treated RGCs and compared to AAV2-GFP/gCOMET treated RGCs. These results remain inconclusive since GFP/gCOMET expression was low in shRNA PKM- $\zeta$  treated axons and was not present in aPKC- $\lambda$  treated axons (Figure 9). Infection will be assessed histologically in the corresponding retinas to count RGCs using GFP/gCOMET immunolabeling to identify infected cells and co-labeling with Brn3a to identify total numbers of surviving RGCs. Retinas infected with AAV2 vectors that modulate aPKC isoform levels will be compared to RGCs from Zymosan+AAV2-GFP/gCOMET treated controls as well as AAV2-GFP/gCOMET controls. Knockdown of PKM- $\zeta$  in infected RGCs will be assessed through FACS to substantially conclude that knockdown of PKM- $\zeta$  does not promote regeneration of RGC axons after optic nerve crush.

Modulating aPKC levels in RGCs may not be neuroprotective or may actively promote cell death, and may be the source of the phenomena seen in aPKC treated optic nerves after crush. If modulating aPKC levels in RGCs is not neuroprotective, we would predict that we would not see an effect on regeneration after treatment since RGCs typically degenerate and die after injury. Alternatively, modulating aPKC levels may promote cell death in RGCs and not DRGs which might reflect differences in NF $\kappa$ B signaling between RGCs and DRGs which is activated downstream of aPKC-Par complexes in different cell types [54] [55]. To address this question in the future, combinatorial treatments will be performed where we will combine aPKC modulation treatments with known neuroprotective and pro-regenerative treatments, like lens

injury or PTEN knockdown, to test for synergistic effect [53] [20]. Modulating these aPKC isoforms have also been tested in injured CST neurons since these CNS neurons do not undergo programmed cell death upon injury.

#### *Regeneration of CST Axons after C4 Dorsal Column Lesion and E14 Graft*

Due to differences in GFP/gCOMET labeling between the shRNA treated and control groups, re-quantification will be needed to determine if any enhancement of or inhibition of axon growth after treatment with shRNA against PKM- $\zeta$  was observed. Regeneration of CST after aPKC- $\lambda$  treatment remains inconclusive due to lack of GFP/gCOMET expression in both the cortex and the CST axons (Figure 11, Figure 12). Lack of GFP/gCOMET expression by the AAV2-aPKCi-GFP virus in the CST is consistent with lack of GFP/gCOMET expression in the optic nerve. Assessment of viral infection will be done to test whether or not the viral treatment is infecting the cells or if the cells are dying upon infection.

CST treatment with shRNA against PKM- $\zeta$  also revealed lower GFP/gCOMET expression and less infection than the GFP/gCOMET control virus. Assessment of viral infection or viral toxicity will also be done for this treatment. This decrease in GFP/gCOMET expression may have resulted in underrepresentation of infected CST axons, qualitatively and quantitatively. Future quantification of growth into the graft will be done normalizing GFP/gCOMET expression into the graft with GFP/gCOMET expression just outside of the graft to account for variability in virus transduction.

. Similar to in the retina, modulating aPKC levels may promote cell death in CST neurons by affecting NF $\kappa$ B pro-apoptotic signaling [54] [55]. Analysis of the

effect of treatment on NF $\kappa$ B and other pro-apoptotic markers will be performed to account for any potential toxicity of these treatments.

Alternatively, the shRNA against PKM- $\zeta$  may not be successfully knocking down PKM- $\zeta$  in the cortical neurons. Confirmation of PKM- $\zeta$  knockdown in CST neurons must be assessed to connect phenotype with treatment. Additionally, the shRNA construct may have off-target effects that may be detrimental to either the health of the cortical neurons or to the regenerative ability of the CST axons. Analysis of the levels of other aPKC isoforms also will be performed to assess for off-target effects of the shRNA construct.

## **Future Directions: Hypothesis-Driven Candidate Approach**

### *Repeat DRG Neurite Outgrowth Assays*

PKM- $\zeta$ , aPKC- $\lambda$  and the shRNA sequence targeting PKM- $\zeta$  were all cloned into backbones with a GFP/gCOMET fluorescent reporter to promote consistent fluorescent expression and analysis for future repeats of this assay (Table 3). They have also been made into Lentiviral vectors for increased cell expression for *in vitro* repeats as well as for the experiment discussed below.

### *Confirmation of shRNA Specificity*

Experiments to confirm successfully and specific knockdown of PKM- $\zeta$  in DRGs as well as in RGCs are underway. AAV2 infected rat RGCs will be dissociated from adult rat retinas and sorted through FACS for GFP+ cells, indicating successful infection, one week after infection. The RNA from these sorted GFP+ cells will be isolated and RT-qPCR will be performed to assess relative levels of PKM- $\zeta$ , aPKC- $\zeta$ , and aPKC- $\lambda$  mRNA compared to GAPDH mRNA. More retinas will be used and properly dissociated to a single cell suspension to ensure that enough cells can be collected post-FACS to yield enough RNA for analysis. Additionally, more wells of infected DRGs will be pooled per treatment to also ensure high yield of RNA for proper analysis.

### *Combinatorial Treatments In Vitro and In Vivo*

A plasmid expressing aPKC- $\lambda$  and dTomato/rCOMET, a red fluorescent reporter, was cloned and AAV2 has been made for combinatorial treatments with shRNA PKM- $\zeta$  GFP/gCOMET plasmid or virus. Neurite outgrowth can be analyzed

using a double-positive analysis program after combinatorial treatment with both aPKC- $\lambda$  and shRNA against PKM- $\zeta$  in adult DRGs cultured on an inhibitory substrate. These experiments are currently underway. If significant neurite outgrowth is observed, *in vivo* combinatorial treatments in both the rat optic nerve crush model and in rat dorsal column lesion and graft models will be performed.

#### *Assessment of RGC Survival Post-Infection*

Immunohistochemistry will be performed on histological sections of the retinas from the optic nerve crush experiment discussed previously. A count of the number of infected RGCs by GFP/gCOMET expression compared to total RGCs by Brn3a expression will reveal the rate of infection by our AAV2 stocks but also any potential death caused by our viral treatments compared to both Zymosan and AAV2 control treated RGCs, including values from retinas with corresponding crushed or uncrushed optic nerves. A dosage experiment should also be performed to assess whether or not constant increased expression of aPKC- $\lambda$  or knockdown of PKM- $\zeta$  can be harmful to RGCs over time.

#### *Assessment of AAV2- aPKC- $\lambda$ Titer and Infection of RGCs and CST Neurons*

Infected retinal ganglion cells will be counted and compared to the number of alive and Brn3a positive RGCs to assess for any effect on RGC survival after treatments. Infected cortical neurons will also be counted and compared to the number of NeuN positive neurons in the cortex to assess for any effect on cortical neuron survival after treatment. Additional *in vitro* experiments will be performed

involving the infection of primary neuronal cell lines by various titers of each virus to assess for viral titer and toxicity.

#### *Quantification and Repeats of In Vivo Experiments*

Quantification of axon regeneration in the optic nerve crush experiment is underway. Axons in the optic nerve traced by CTB as well as axons traced by GFP/gCOMET expression (representing infected axons) are being counted per area in all treatments. Repeats of the above optic nerve crush experiments and dorsal column lesion experiments in rats will be repeated with functionally validated AAV2 vectors to verify physiological effect. In the optic nerve crush experiments, a growth factor (e.g. CNTF) that provides robust neuroprotection to RGCs, will be injected into the vitreous after injection of the virus as well as immediately after optic nerve crush to promote RGC survival. This should separate any pro-regenerative effects of aPKC- $\lambda$  and knockdown of PKM- $\zeta$  from injury and treatment induced cell death. This will be necessary if our histological results from infected retinas demonstrate RGC death after infection with either aPKC- $\lambda$  or shRNA-PKM- $\zeta$  expressing AAV2 vectors.

The quantification of CST fibers regenerating into E14 NSC grafts will also be re-evaluated by counting the fibers in the main CST tract at increasing distances from the rostral/host-graft border, and normalizing the numbers of fibers in the graft to this labeled fiber density. This quantification technique will better account for any differences in analysis based on differences in GFP/gCOMET fluorescence intensity.

Also, optic nerve crush and dorsal column lesion experiments will be performed on rats post co-infection with AAV2 expressing aPKC- $\lambda$  and dTomato/rCOMET as well as with AAV2 expressing shRNA against PKM- $\zeta$  and

GFP/gCOMET to assess the combined effect *in vivo*. Additionally, optic nerve crush and dorsal column lesion experiments should be performed on rats post infection with AAV2 overexpressing PKM- $\zeta$ . From the *in vitro* DRG experiments, we would anticipate that overexpression of PKM- $\zeta$  would be strongly inhibitory to regenerating axons and would confirm the importance of aPKC mediated downstream signaling on the regulation of axon regeneration following CNS injury.

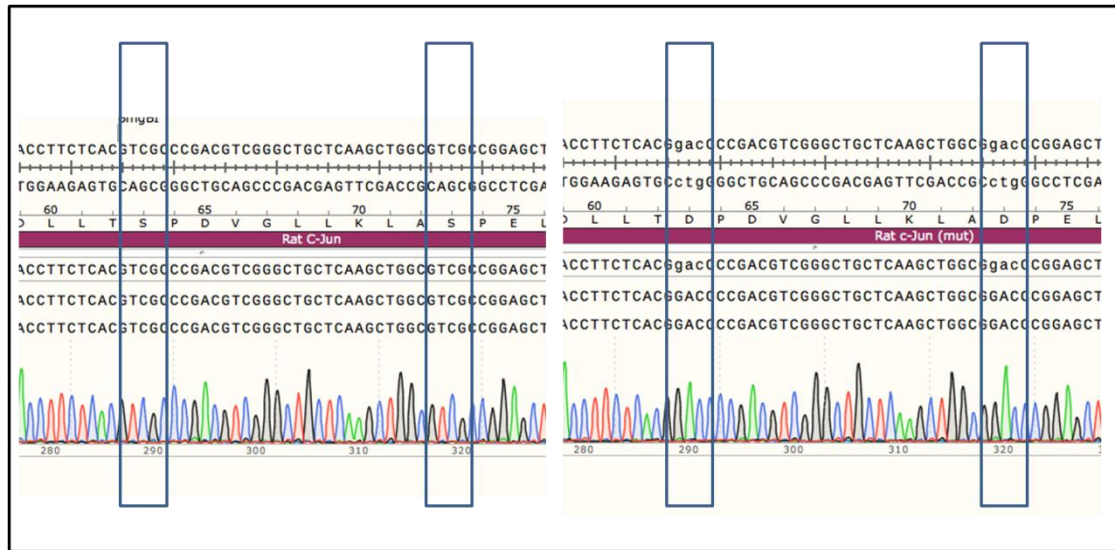
#### *Optic Nerve Crush and Dorsal Column Lesions in Prkcz<sup>-/-</sup> Mice*

*Prkcz<sup>-/-</sup>* mice as well as conditionally deleted *Prkcz* “floxed” (*Prkcz<sup>f/f</sup>*) mice will be used for future experiments to assess the regeneration of both RGC axons and CST axons in animals lacking aPKC- $\zeta$  as well as PKM- $\zeta$ , in constitutive null mice or in specific cell types by utilizing post-natal Cre-induced knockout of the gene.

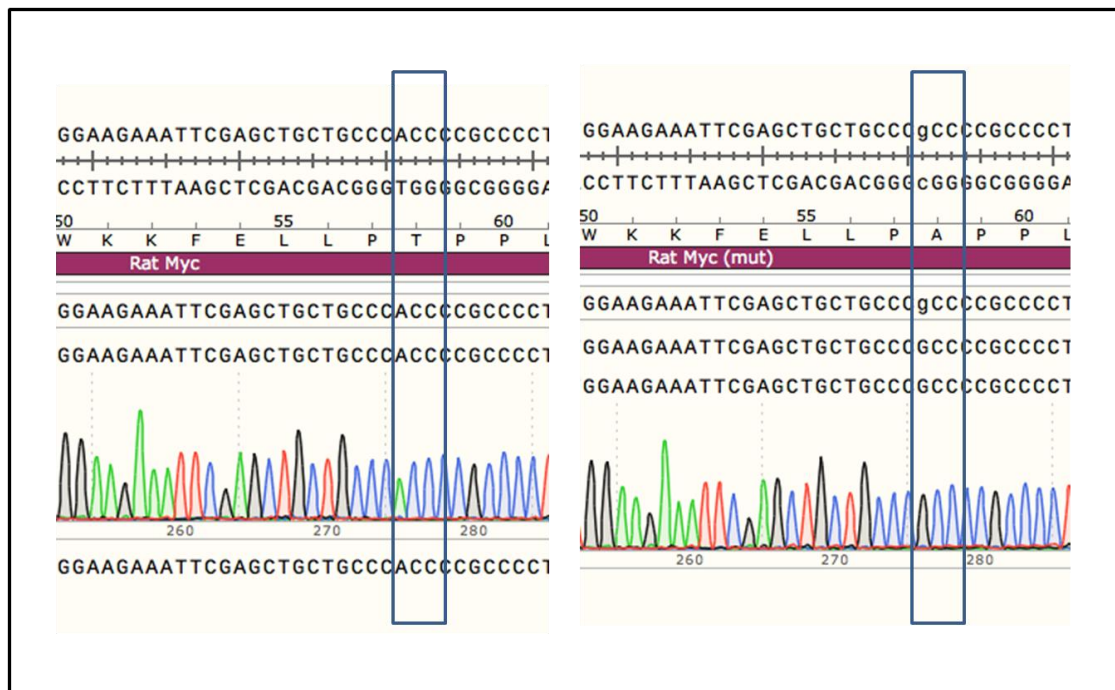
#### *Sciatic Nerve Crush and Assessment of PNS Regeneration*

Since positive results were seen in DRGs, a PNS cell type, we plan on testing the effect of both overexpressing aPKC- $\lambda$  and knocking down PKM- $\zeta$  in sciatic nerve crush model to assess for influence on PNS regeneration. Our collaborators also showed that levels of PKM- $\zeta$  are higher in the DRG peripheral axon compared to the central axon and soma combined, leading us to hypothesize that PKM- $\zeta$  may have a significant role in PNS regeneration (Figure 21).

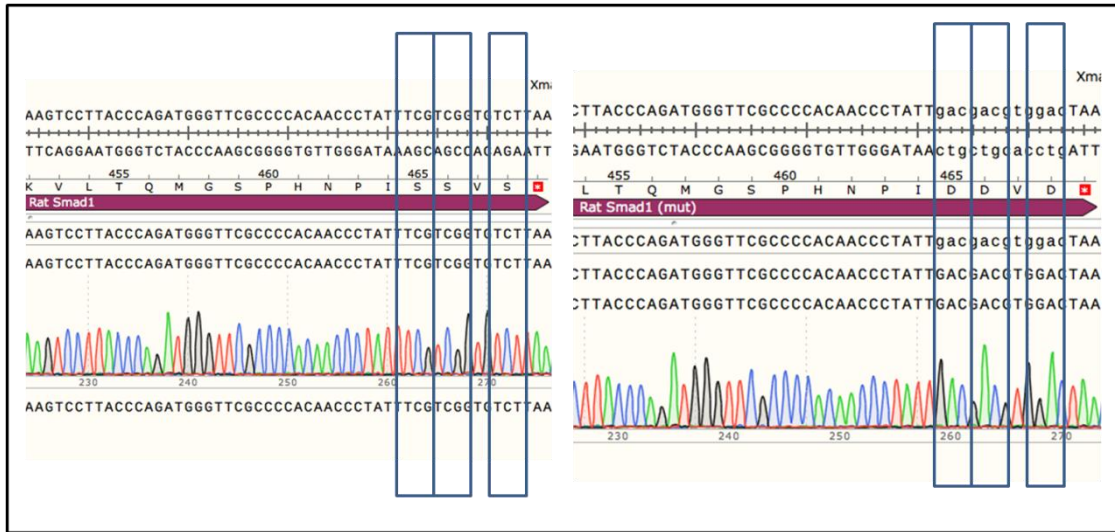
## FIGURES



**Figure 1:** Sequence Comparison of Non-Mutated and Mutated *c-Jun*. Amino acids 63 and 73 were successfully mutated from serine to aspartic acid by replacing the nucleotide sequence TCG (5' to 3') of the original plasmid to GAC (5' to 3').



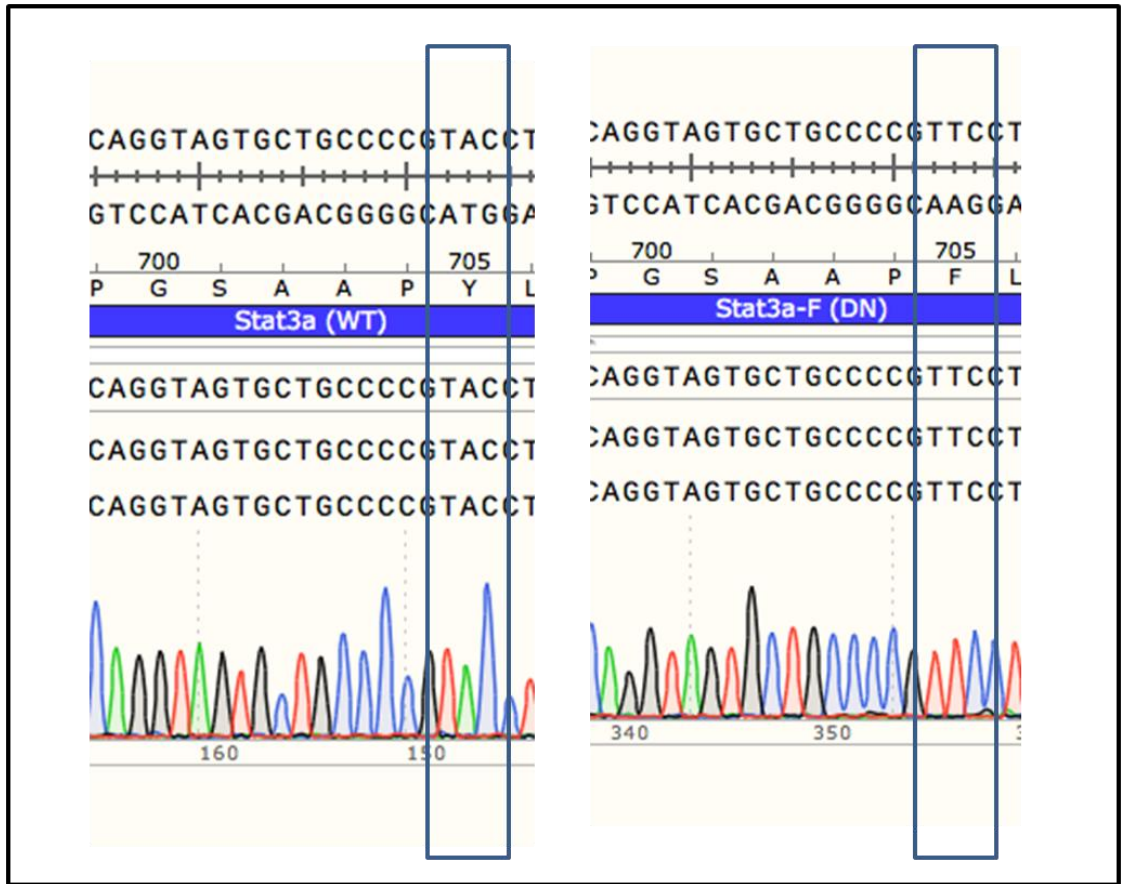
**Figure 2:** Sequence Comparison of Non-Mutated and Mutated *Myc*. Amino acid 58 was successfully mutated from a threonine to an alanine by replacing the nucleotide sequence ACC (5' to 3') of the original plasmid to GCC (5' to 3').



**Figure 3:** Sequence Comparison of Non-Mutated and Mutated Smad1. Amino acids 465, 466, and 468 were successfully mutated from serine to aspartic acid by replacing the nucleotide sequence TCG and TCT (5' to 3') of the original plasmid to GAC (5' to 3').

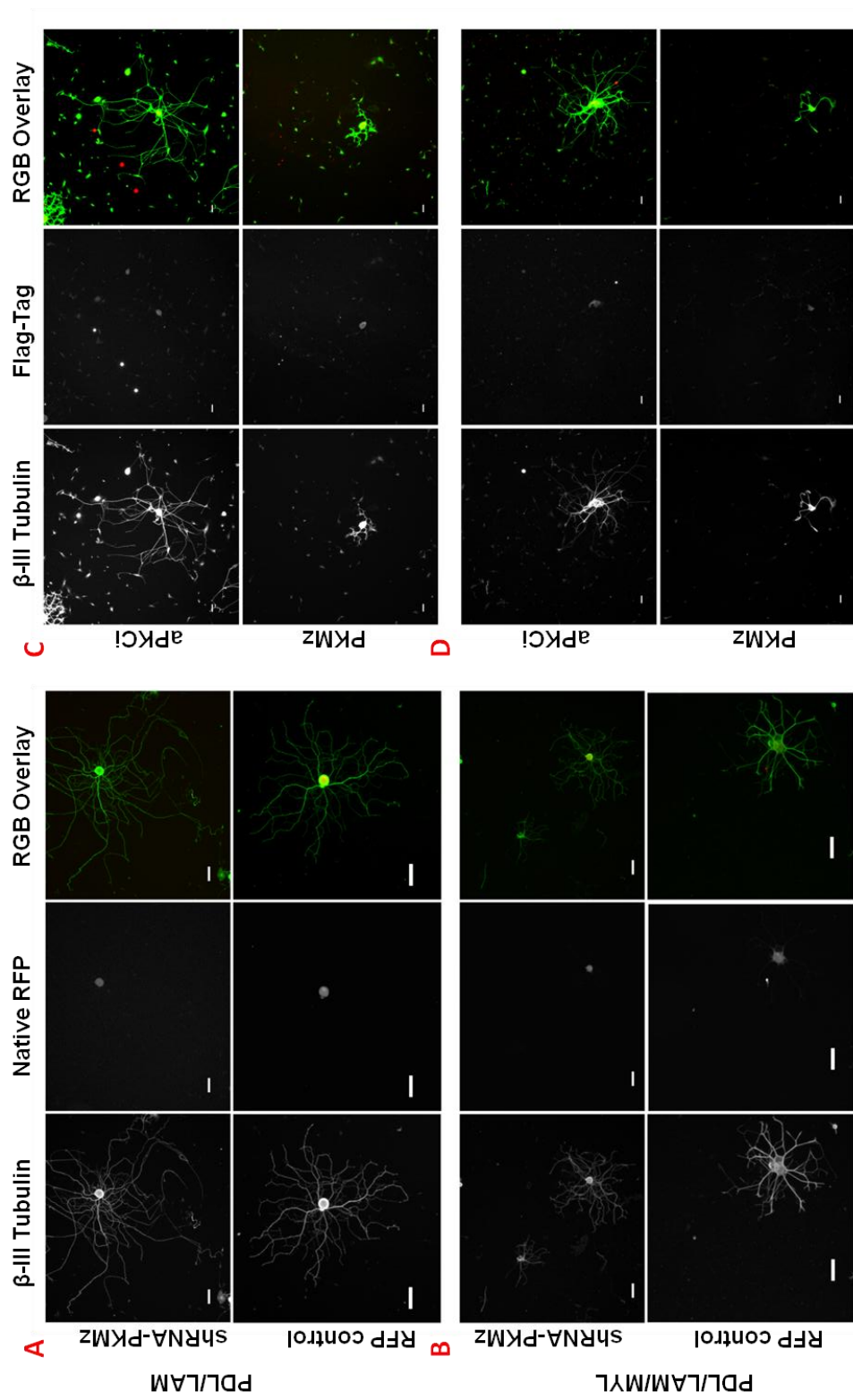


**Figure 4:** Sequence Comparison of Wild Type and Constitutively Active Stat3a. Amino acids 662 (661) and 664 (663) had previously been mutated from an alanine and asparagines, respectively, to cysteines by replacing the nucleotide sequence GCG and AAC (5' to 3') of the original plasmid to TGT and TGC (5' to 3'), respectively.



**Figure 5:** Sequence Comparison of Wild Type and Dominant Negative Stat3a. Amino acid 705 had been previously mutated from tyrosine to phenylalanine by replacing the nucleotide sequence TAC (5' to 3') of the original plasmid to TTC (5' to 3').

**Figure 6: Characteristic Images of Transfected DRGs on Various Substrates. A)** Images showing  $\beta$ -III Tubulin and native RFP (tdTomato and RFP) expression and an RGB overlap of DRGs transfected with either pLeGO-U6-shRNA-PKMz-SSFV-tdTomato (shRNA PKMz) or pRRL-ppt-CAG-RFP-WPre (RFP control) plated on poly-D-lysine and laminin (PDL/LAM) **B)** Images showing DRGs similarly transfected to A, plated on poly-D-lysine, laminin, and myelin (PDL/LAM/MYL) **C)** Images showing  $\beta$ -III Tubulin and Flag-tag expression and an RGB overlap of DRGs transfected with either pSG-290-3xFlag-aPKCi (aPKCi) or pCMV-3xFlag-PKMz (PKMz) plated on PDL/LAM **D)** Images showing DRGs similarly transfected to C, plated on PDL/LAM/MYL. All scale bars are 100 $\mu$ m in length.



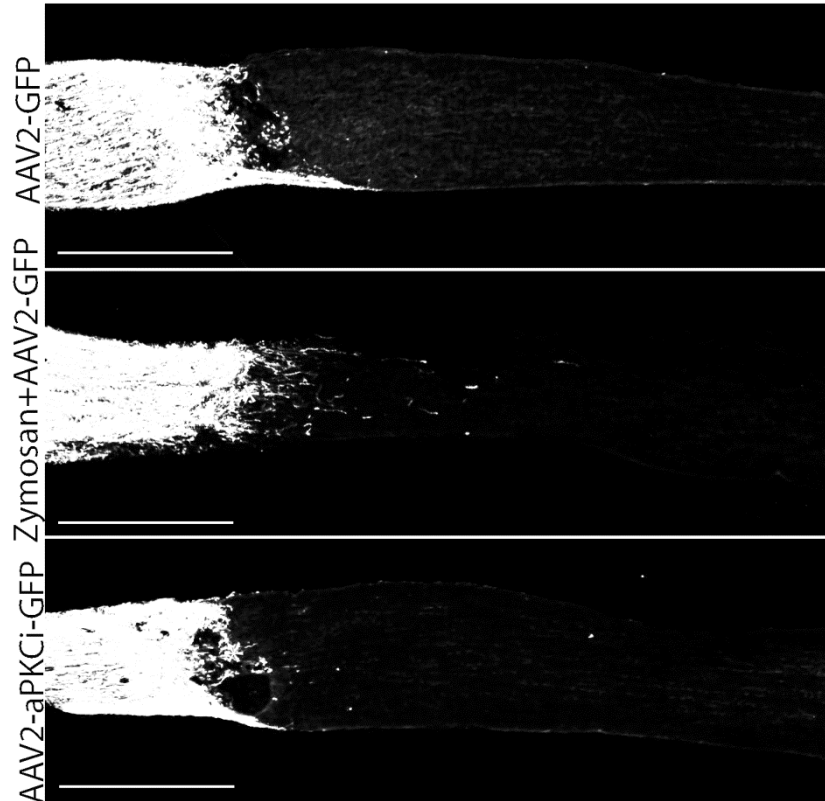


**Figure 7:** Cholera Toxin B Staining of AAV2 aPKCi Treated Optic Nerves After Crush. Scale bar = 500 $\mu$ m. (From top to bottom) AAV2-GFP/gCOMET treated optic nerve as negative control of regeneration Zymosan and AAV2-GFP/gCOMET treated optic nerve as positive control. AAV2- aPKCi-GFP/gCOMET treated optic nerve. Grayscale images of CTB staining. Asterisks represent distal end of crush site used for quantification of regeneration.

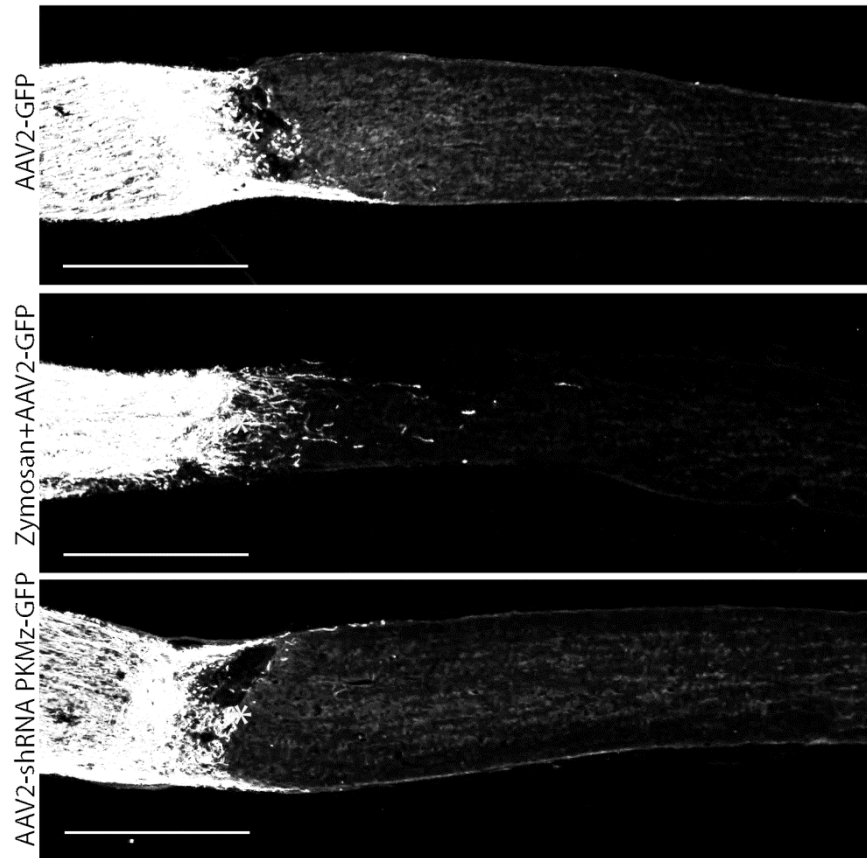


**Figure 8:** Cholera Toxin B Staining of AAV2 shRNA PKMz Treated Optic Nerves After Crush. Scale bar = 500 $\mu$ m. (From top to bottom) AAV2-GFP/gCOMET treated optic nerve as negative control of regeneration Zymosan and AAV2-GFP/gCOMET treated optic nerve as positive control. Two AAV2- shRNA PKMz-GFP/gCOMET treated optic nerve. Grayscale images of CTB staining. Asterisks represent distal end of crush site used for quantification of regeneration.

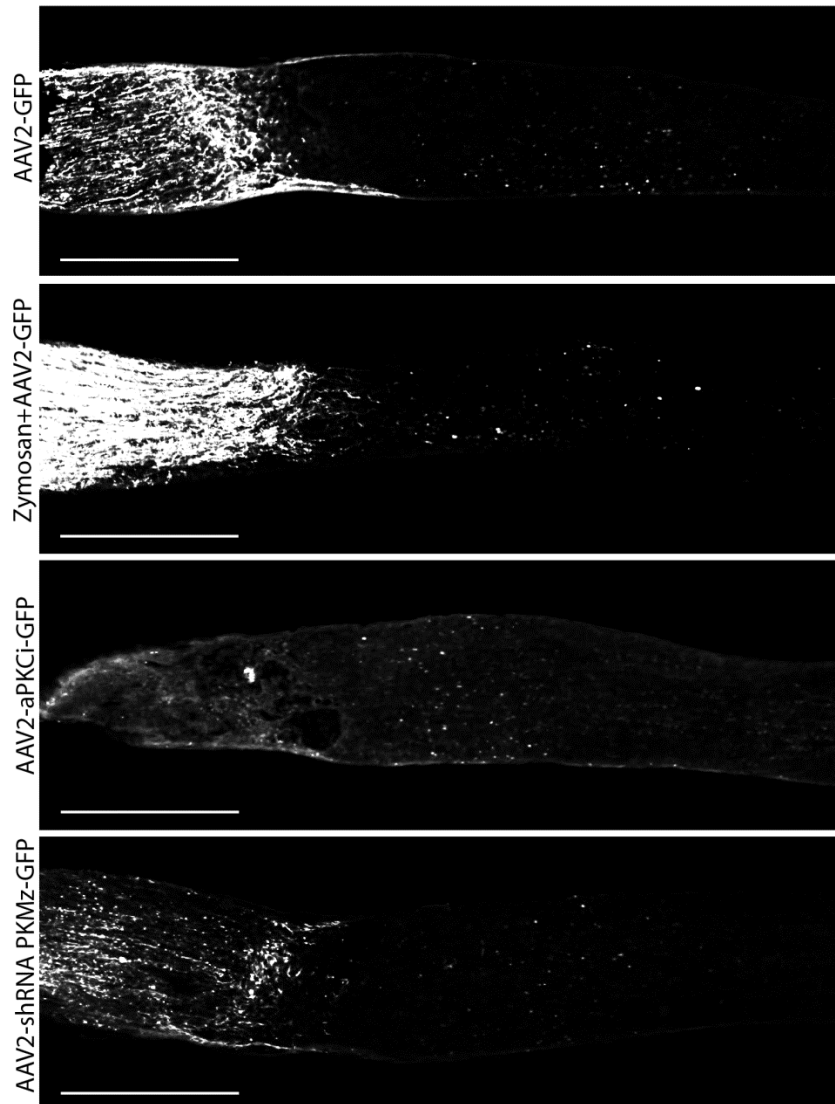


**Figure 9:** *GFP/gCOMET Staining of Representative Optic Nerve Sections After AAV2 Injection and Crush.* Scale bar = 500 $\mu$ m. (From top to bottom) AAV2-GFP/gCOMET treated optic nerve as negative control of regeneration. Zymosan and AAV2-GFP/gCOMET treated optic nerve as positive control. AAV2-aPKCi-GFP/gCOMET treated optic nerve. AAV2- shRNA PKMz-GFP/gCOMET treated optic nerve. Grayscale images of GFP/gCOMET staining. Images show the optic nerve both proximal and distal to the lesion site.

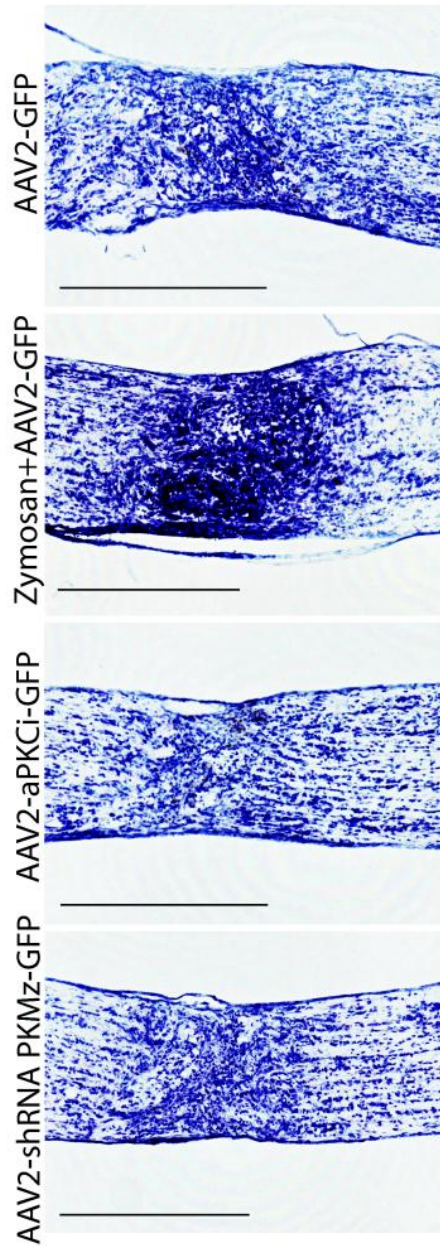


**Figure 10:** *Nissl Staining of Representative Optic Nerve Sections to Assess Consistency of Crush.* Scale bar = 500 $\mu$ m. Crush site of optic nerve sections after various treatments and labeled with Nissl staining to observe morphology of crush site.

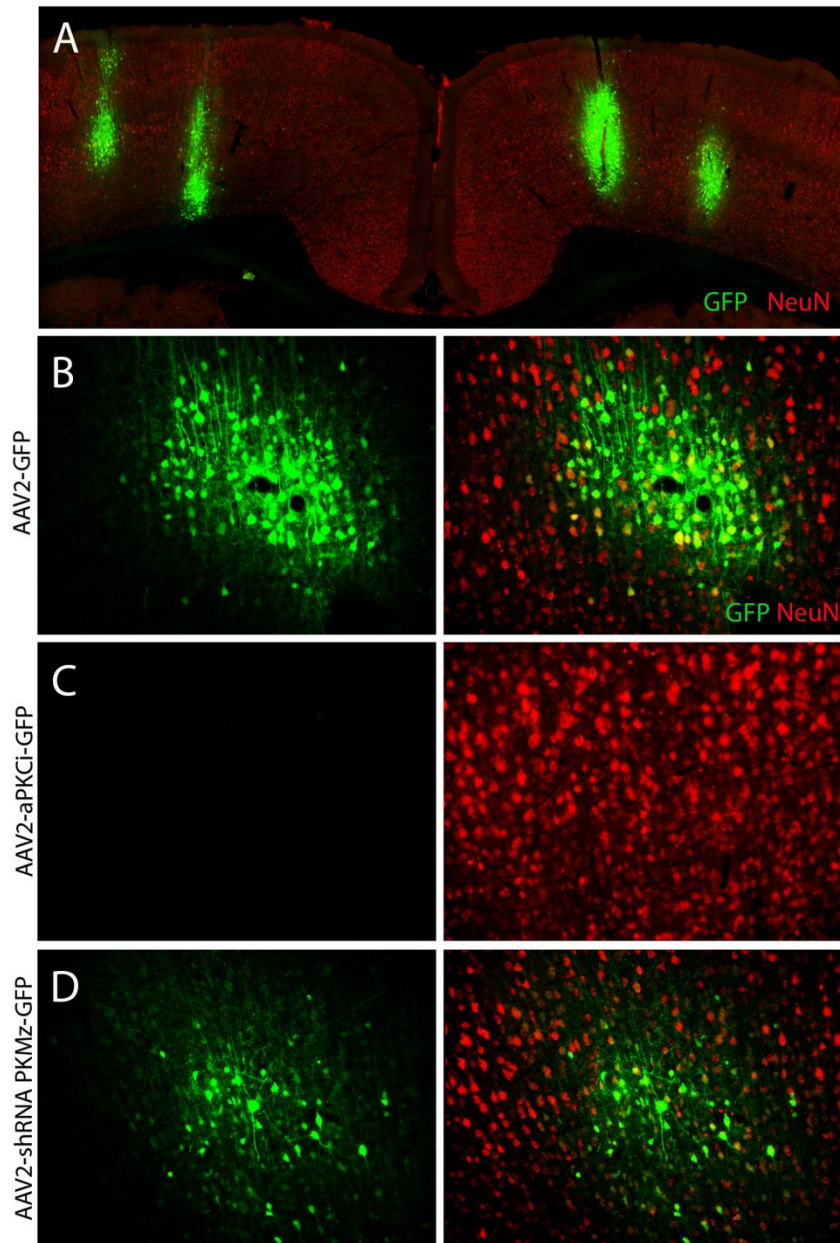


**Figure 11:** *Infection of Cortical Neurons by AAV2.* A) Coronal brain section of the cortex showing GFP labeled neurons in and around layer 5b of the cortex, revealing successful infection of those cortical neurons. B) GFP positive AAV2-GFP infected cortical neurons (left panel) co-labeled with NeuN (right panel) C) Lack of GFP positive AAV2-aPKCi-GFP infected cortical neurons (left panel) and NeuN labeled cortical cells (right panel) D) GFP positive AAV2-shRNA PKMz-GFP treated cortical neurons (left panel) co-labeled with NeuN (right panel).

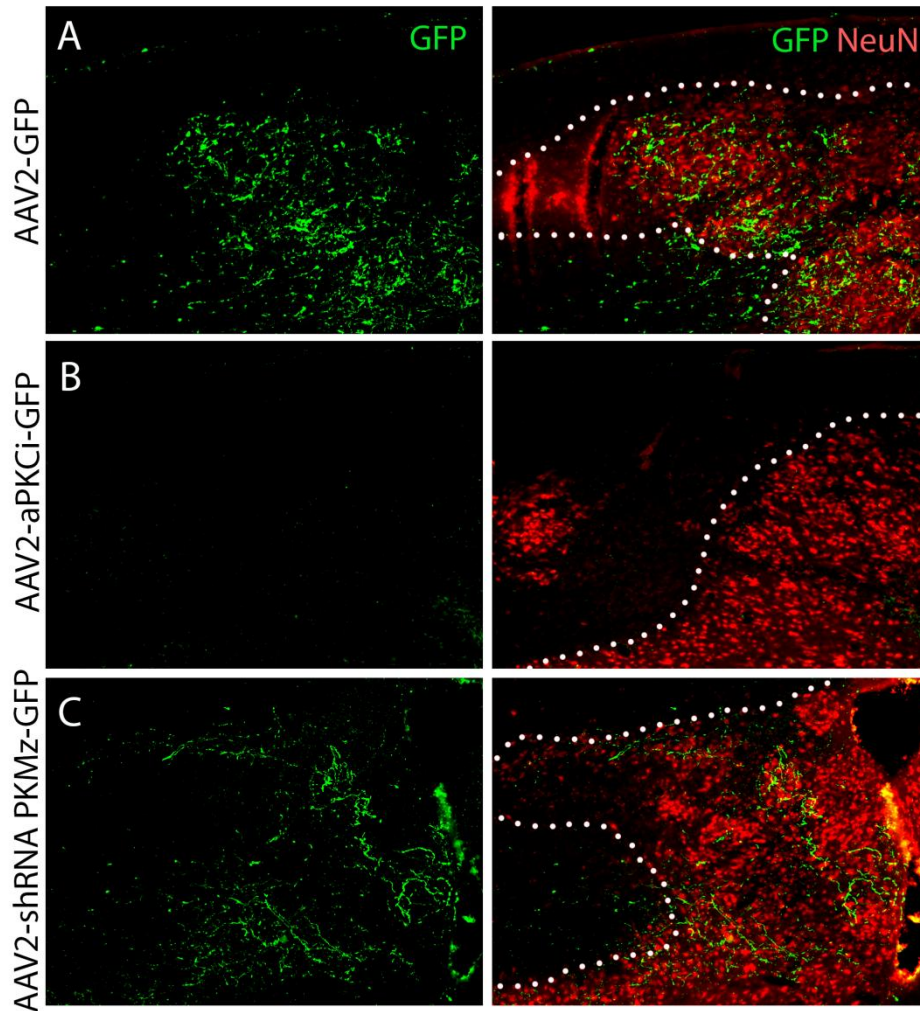


**Figure 12:** *Regenerating CST Fibers into E14 Graft after AAV2 Treatment.* A) GFP positive AAV2-GFP treated CST fibers (left panel) entering NeuN positive E14 graft (right panel) B) Lack of GFP positive AAV2-aPKCi-GFP treated CST fibers (left panel) entering NeuN positive E14 graft (right panel) C) GFP positive AAV2-shRNA PKMz-GFP treated CST fibers (left panel) entering NeuN positive E14 graft (right panel).

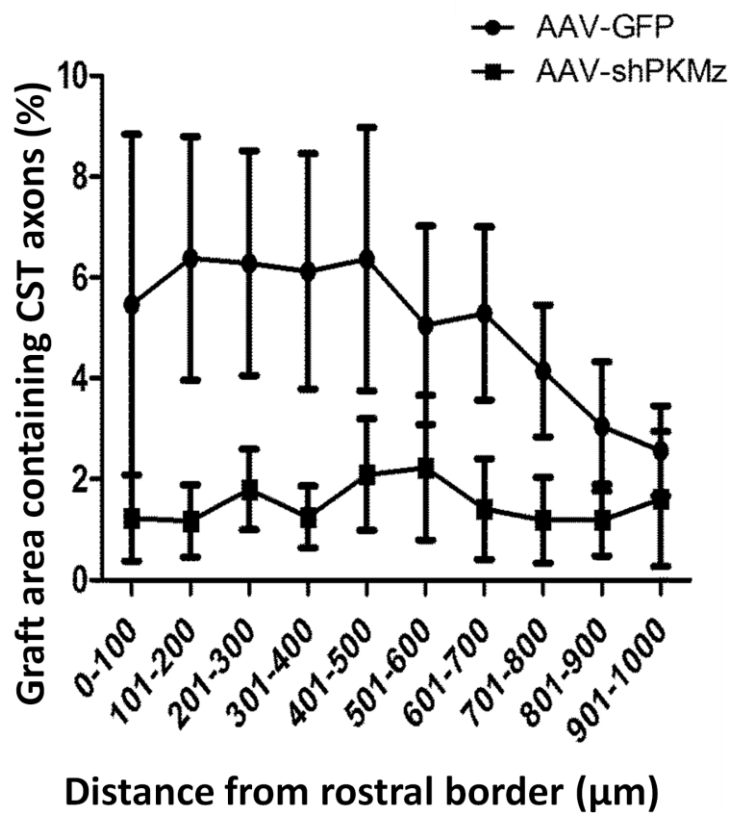


**Figure 13:** Quantification of CST Axon Regeneration into E14 Grafts after AAV2 Treatments. AAV2-aPKCi-GFP treatment was not quantified due to lack of infection and/or GFP expression in cortical neurons. Percentage of the graft area containing GFP+ CST axons at increasing distances from the rostral/host border of the graft of AAV2-GFP (AAV-GFP) treated CST and AAV2-shRNA PKMz-GFP (AAV-shPKMz) treated CST.

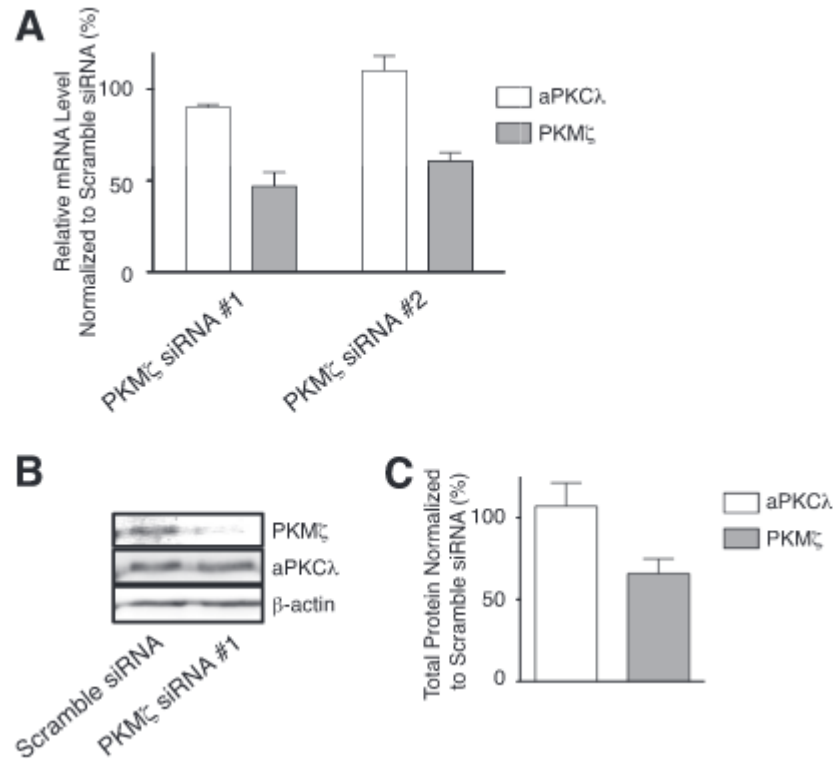
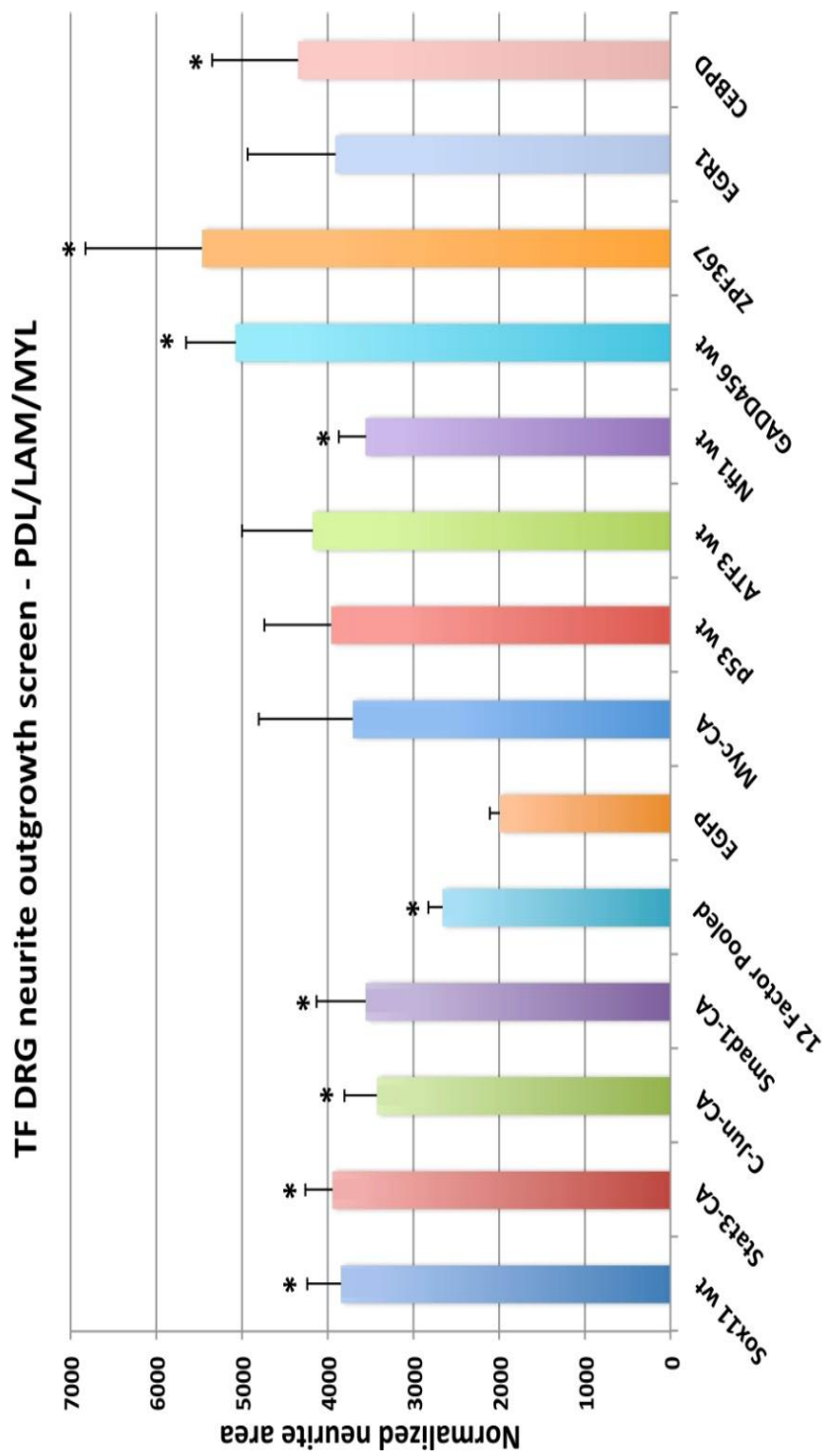


**Figure 14:** Supplemental Figure S2 from Parker SS, et al. (PNAS 2013) **A)** Successful decrease of PKM- $\zeta$  mRNA expression in rat embryonic hippocampal neurons and lack of aPKC- $\lambda$  knockdown in the treated samples. More expression of both isoforms is seen with the treatment of PKM- $\zeta$  siRNA2. **B)** Western Blot showing successful and specific knockdown of PKM- $\zeta$  with the siRNA1 compared to scramble siRNA control and compared to aPKC- $\lambda$  and  $\beta$ -actin protein levels. **C)** Total Protein amount of PKM- $\zeta$  and aPKC- $\lambda$  normalized to scramble shRNA.

**Figure 15:** *Initial Transcription Factor Screen with Individual and Combinatorial Treatments.* Total neurite area per representative image of DRGs cultured on myelin (PDL/LAM/MYL) after lentiviral transduction normalized to EGFP treated cells. Conditions notated as “CA” refer to the constitutively active mutated transcription factors previously described and listed in Table 1. Unpaired Student’s t-tests were performed and p-values were determined as follows: Sox11 ( $p = 0.00787$ ), Stat3a-C ( $p = 0.00290$ ), c-Jun ( $p = 0.0218$ ), Smad1 (mut) ( $p = 0.0464$ ) and pooled transcription factors ( $p = 0.0092$ ). (Error bars = SEM, N=4, \* $P < 0.05$ , \*\* $P < 0.01$ ).



t-test. N=4, ±SEM

\* P<0.05 compared to EGFP control

**Figure 16:** *shRNA Knockdown of PKM- $\zeta$  in DRGs Compared to Transfection Control.* Analysis of DRGs treated with shRNA knockdown of PKM- $\zeta$  compared to a control plasmid expressing RFP on three substrates: poly-d-lysine (PDL), laminin (PDL/LAM), and myelin (PDL/LAM/MYL). **A)** Total neurite outgrowth on PDL, PDL/LAM ( $p = 0.0214$ ) and PDL/LAM/MYL ( $p = 0.0444$ ). **B)** Total cell branches on PDL, PDL/LAM ( $p = 0.0366$ ) and PDL/LAM/MYL ( $p = 0.0397$ ). **C)** Number of neurites per cell on PDL ( $p = 0.0410$ ), PDL/LAM ( $p = 0.0144$ ), and PDL/LAM/MYL ( $p = 0.0333$ ). **D)** Maximum process length on PDL, PDL/LAM ( $p = 0.0475$ ), and PDL/LAM/MYL ( $p = 0.0493$ ). (Error bars = SEM, N=3, \* $P < 0.05$ , \*\* $P < 0.01$ , unpaired Student's T-test).

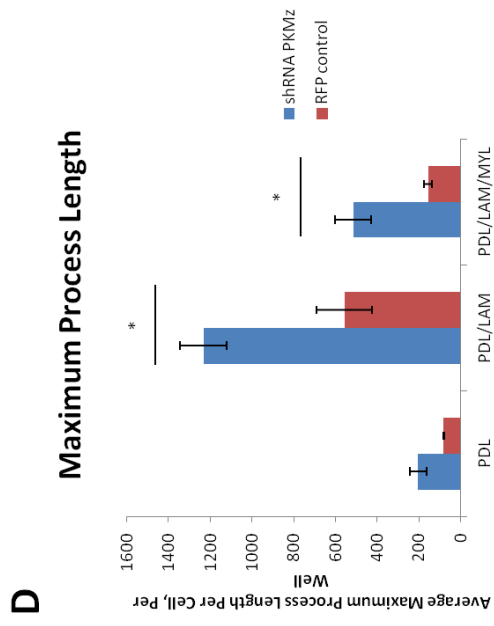
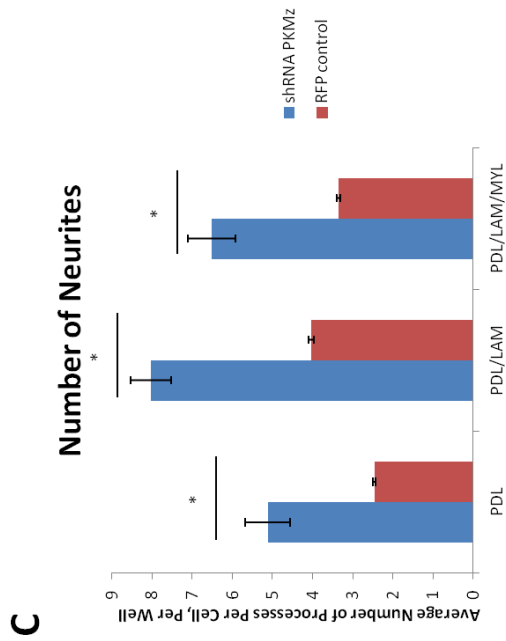
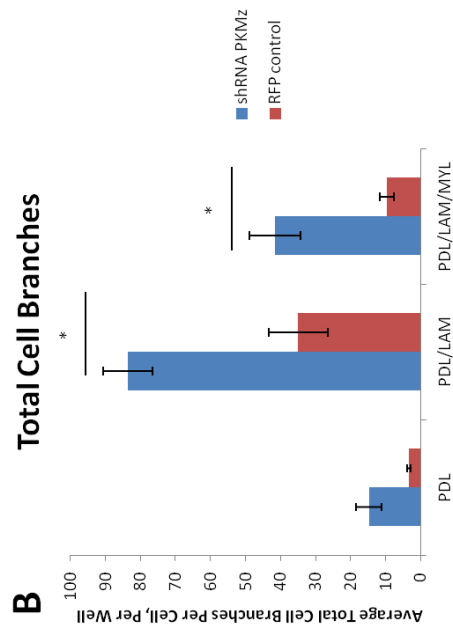
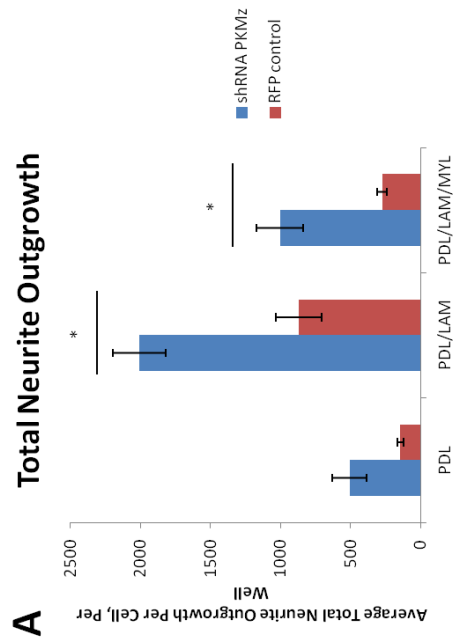
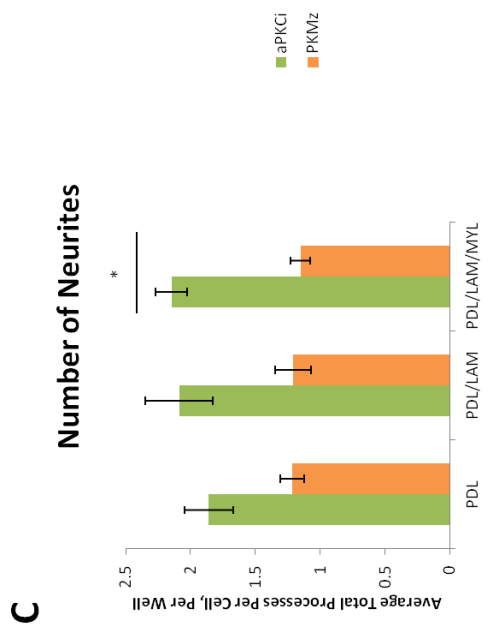
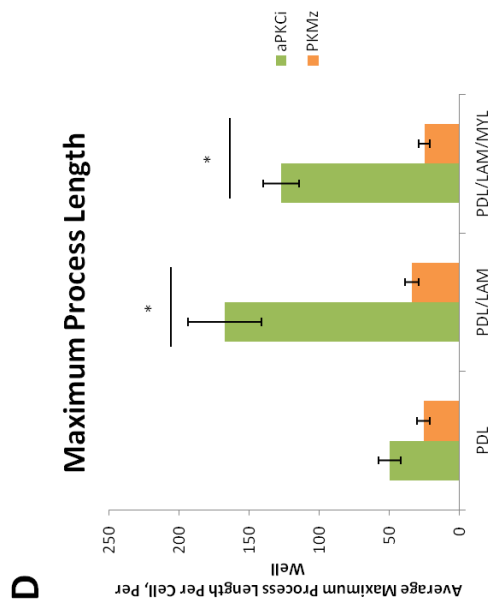
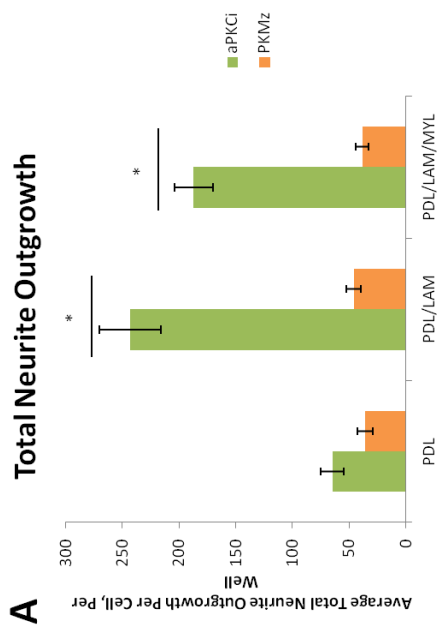
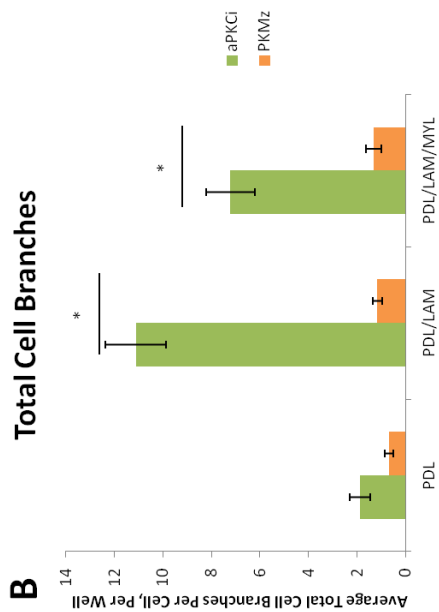


**Figure 17:** *Upregulation of aPKC- $\lambda$  in DRGs Compared to Upregulation of PKM- $\zeta$ .* Analysis of DRGs treated with a plasmid overexpressing aPKC- $\lambda$  compared to DRGs treated with a plasmid overexpressing PKM- $\zeta$  on three substrates: poly-d-lysine (PDL), laminin (PDL/LAM), and myelin (PDL/LAM/MYL). A) Total neurite outgrowth on PDL, PDL/LAM ( $p = 0.0214$ ), and PDL/LAM/MYL ( $p = 0.0444$ ). B) Total cell branches on PDL, PDL/LAM ( $p = 0.0366$ ), and PDL/LAM/MYL ( $p = 0.0397$ ). C) Number of neurites per cell on PDL ( $p = 0.0410$ ), PDL/LAM ( $p = 0.0144$ ), and PDL/LAM/MYL ( $p = 0.0333$ ). D) Maximum process length on PDL, PDL/LAM ( $p = 0.0334$ ), and PDL/LAM/MYL ( $p = 0.0103$ ). (Error bars = SEM, N=3, \* $P < 0.05$ , \*\* $P < 0.01$ , unpaired Student's T-test).



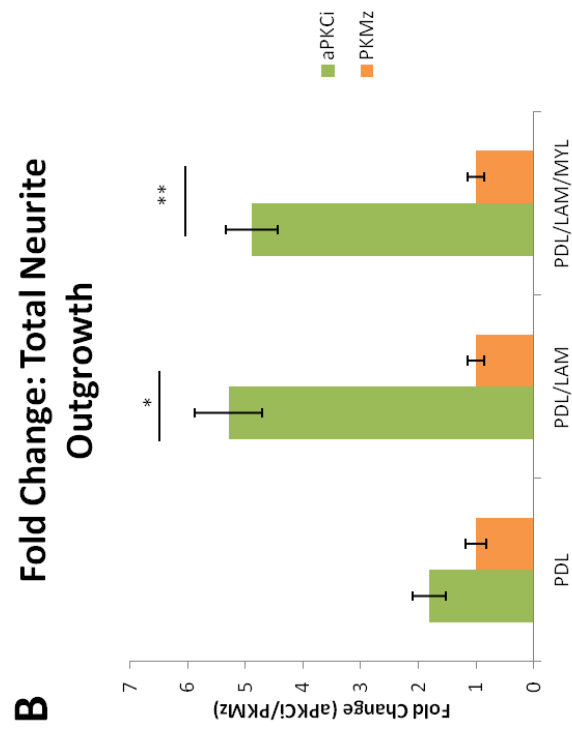
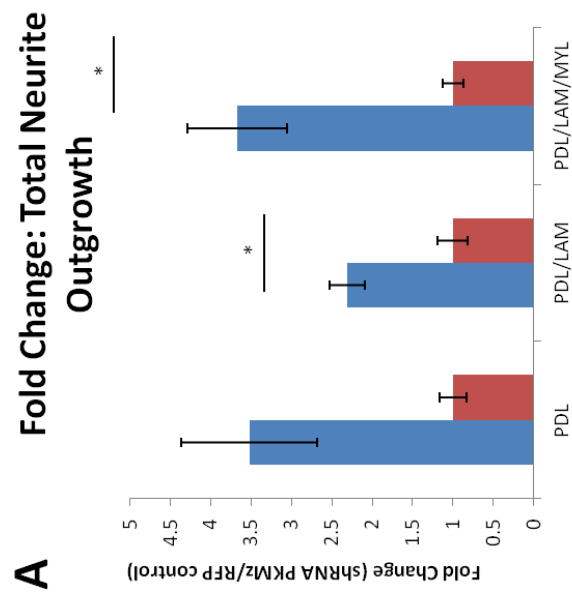
**A**

**B**

**C**

**D**

**Figure 18:** *Fold Change of Total Neurite Outgrowth of shRNA Knockdown of PKM- $\zeta$  and Upregulation of aPKC- $\lambda$  in DRGs.* shRNA knockdown of PKM- $\zeta$  compared to RFP transfection control. Histograms show relative fold changes in total neurite growth or total neurite branches compared to control. (**A, B**). Overexpression of aPKC- $\lambda$  compared to overexpression of PKM- $\zeta$ . Histograms show relative fold changes in total neurite growth or total neurite branching of overexpression of aPKC- $\lambda$  compared to overexpression of PKM- $\zeta$  (**C, D**). (Error bars = SEM, N=3, \*P<0.05, \*\*P<0.01, unpaired Student's T-test).



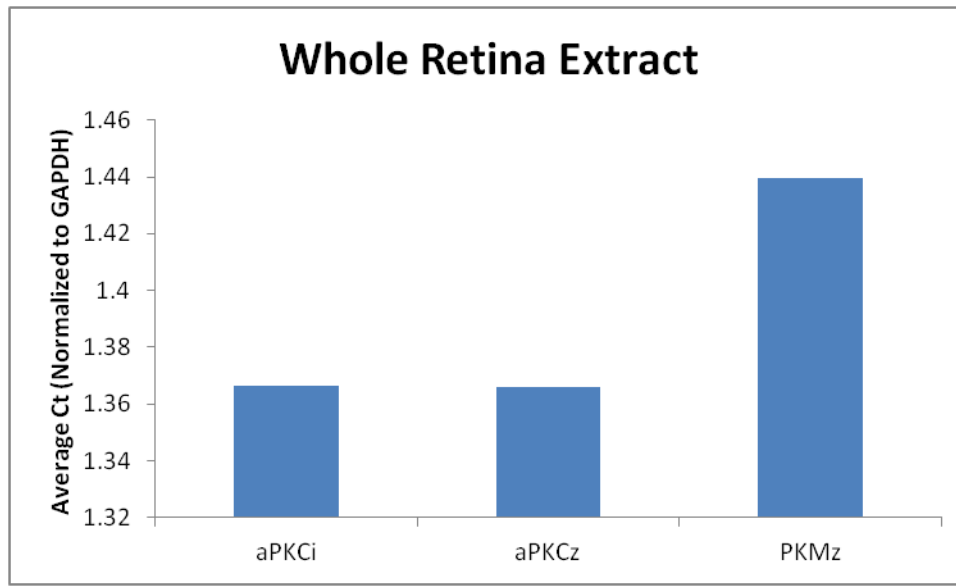


**Figure 19:** RT-qPCR of Whole Rat Retina Extract (Normalized). Average threshold count of aPKC- $\lambda$  (aPKCi), aPKC- $\zeta$  (aPKCz) and PKM- $\zeta$  (PKMz) normalized to GAPDH. n=3 for all samples.

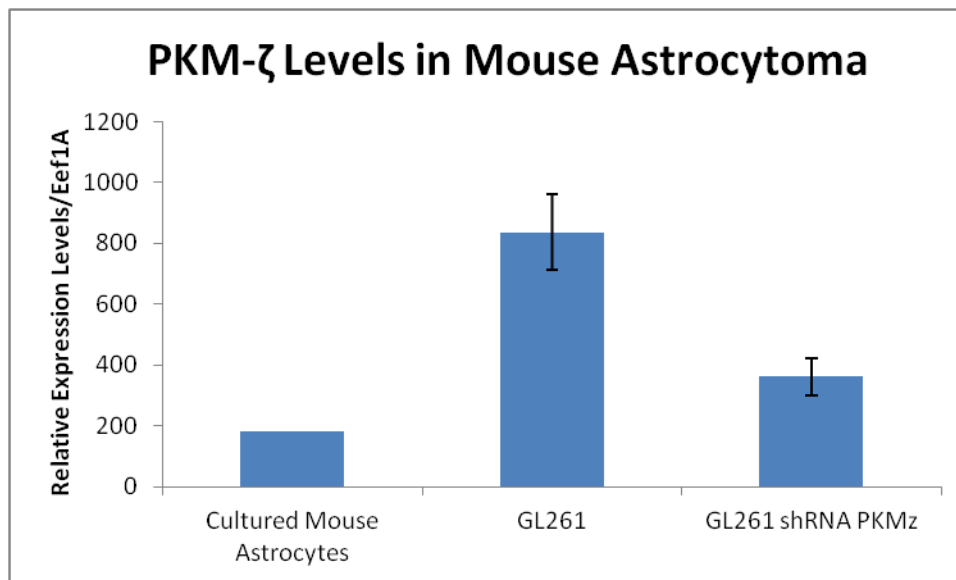


**Figure 20:** Relative Levels of PKM- $\zeta$  in Mouse Astrocytoma. Relative mRNA levels (relative to 1 million copies of the housing-keeping gene Eef1A) in cultured mouse astrocytes, an astrocytoma cell-line (GL261), and GL261 cells treated with shRNA against PKM- $\zeta$ . Replicates are as follows: cultured mouse astrocytes n = 1, GL261 n = 4, GL261 shRNA PKMz n = 3. Error bars = SEM.

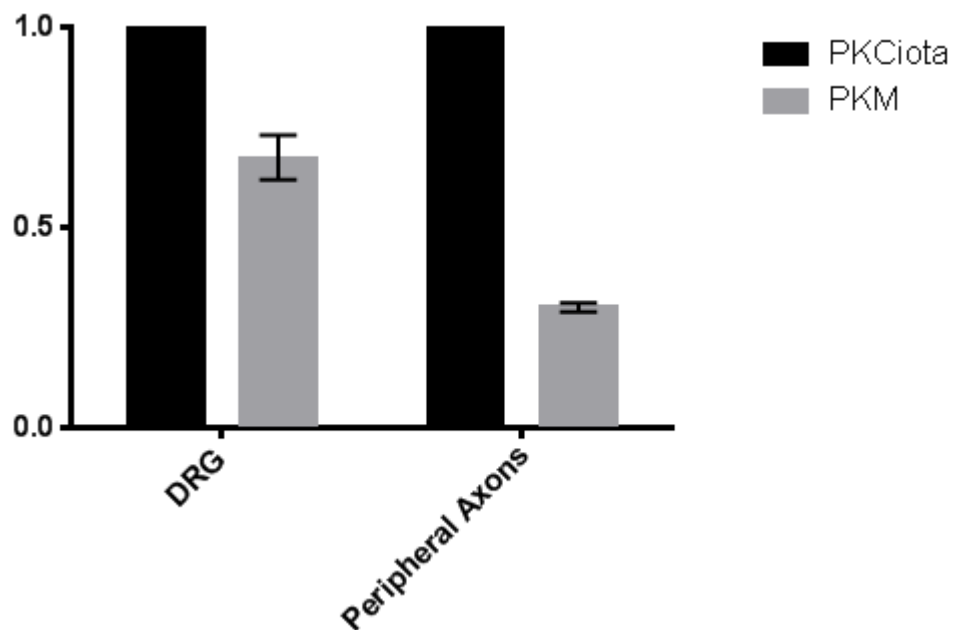


**Figure 21:** *Relative Expression levels of aPKC- $\lambda$  (PKCiota) and PKM- $\zeta$  (PKM) in DRGs and DRG Peripheral Axons.* Unpublished data from collaborator Sourav Ghosh at Yale University showing relative expression levels of both aPKC- $\lambda$  (PKCiota) and PKM- $\zeta$  (PKM) in the central projecting axon of the DRG plus soma (DRG) compared to the peripheral axons of DRGs.

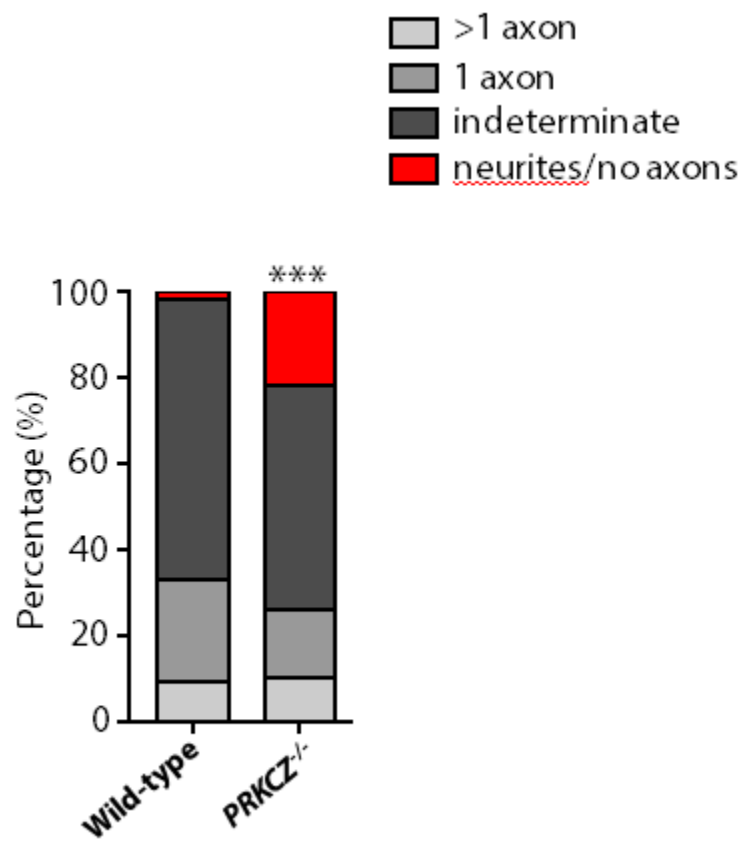


**Figure 22:** Percentage of E18 Hippocampal Neurons with and without Multiple Axons. Unpublished data from collaborator Sourav Ghosh at Yale University showing percentage of neurites in wild-type E18 hippocampal neurons compared to E18 hippocampal neurons of *Prkcz*<sup>-/-</sup> mice.

## TABLES

**Table 1: Site-Directed Mutagenesis Primers.** These primers were produced for the listed transcription factor plasmid constructs from Table 2 to mutate the wild type sequence to a constitutively active form.

Transcription Factor	SDM Primer 1	SDM Primer 2
c-Jun	tcggaccttctcacggacccccgacgtcgggctg ctcaagctggcggacccggagctggagcgc	gcgctccagctccgggtccgcc agcttgagcagcccgacgtcgg ggctccgtgagaaggtccga
Myc	agctgctgccgcccccgccctg	caggggcggggcgggcagca gct
Smad1	cttaccagatgggttcgccccacaaccctattg acgacgtggactaactcgagatatctagaccca gctttctg	caagaaagctgggtctagatatac tcgagttagtcacgtcgtcaata gggtgtggggcgaaccatctg ggtaag

**Table 2: Plasmids used in Unbiased Candidate Approach.** These plasmids were either obtained from previous lab members or cloned into a consistent lentiviral backbone expressing the same green fluorescent reporter (GFP/gCOMET). The constructs highlighted in yellow were used as templates for site-directed mutagenesis to produce the plasmid constructs highlighted in blue.

pRRL-CMV-gCOMET-p53	pRRL-CMV-gCOMET-ZFP367
pRRL-CMV-gCOMET-ATF3	pRRL-CMV-gCOMET-Sox11
pRRL-CMV-gCOMET-cJun	pRRL-CMV-gCOMET-CEBPD
pRRL-CMV-gCOMET-GADD45g	pRRL-CMV-gCOMET-Stat3a-C
pRRL-CMV-gCOMET-EGR1	pRRL-CMV-gCOMET-Stat3a-F (DN)
pRRL-CMV-gCOMET-Nfil	pRRL-CMV-gCOMET-Stat3a (WT)
pRRL-CMV-gCOMET-Myc	pRRL-CMV-gCOMET-Smad1
pRRL-CMV-gCOMET-cJun (mut)	pRRL-CMV-gCOMET-Myc (mut)
pRRL-CMV-gCOMET-Smad1 (mut)	

**Table 3: Plasmids used in Biased Candidate Approach.** These plasmids were used in the *in vitro* and *in vivo* experiments of the Biased Candidate Approach project. The highlighted plasmids were supplied by Dr. Ghosh and his laboratory at Yale University. All other constructs were cloned from the original highlighted plasmids into either a lentiviral plasmid or an adeno-associated viral backbone to maintain consistency of expression of both the gene of interest and the fluorescent reporter.

pCMV-3xFlag-PKMz	pLeGO-U6-shRNA PKMz-SSFV-tdTomato
pSG-290-3xFlag-aPKCi	pSG-408-LeGO-3xFlag-aPKCi-IRES2-tdTomato
pRRL-CMV-gCOMET-U6-shRNA PKMz	pAAV-CAG-gCOMET-U6-shRNA PKMz
pRRL-CMV-gCOMET-3xFlag-PKMz	pAAV-CAG-gCOMET-3xFlag-PKMz
pRRL-CMV-gCOMET-3xFlag-aPKCi	pAAV-CAG-gCOMET-3xFlag-aPKCi
pRRL-CMV-rCOMET-3xFlag-aPKCi	pAAV-CAG-rCOMET-3xFlag-aPKCi
	pAAV-CAG-gCOMET-U6-scramble shRNA

**Table 4: RT-qPCR Primers.** These primers were designed by Sarah Parker and Sourav Ghosh previously at Arizona State University and used for RT-qPCR to confirm specificity of PKM- $\zeta$  knockdown in adult DRGs and RGCs.

Gene (Rat)	Primer Sequence
GAPDH	AGGTCGGTGTGAACGGATTTG
	GGGTCGTTGATGGCAACA
Eef1A	TGCCAATTTCTGGTTGGAATG
	GGGTGACTTTCCATCCCTTGA
Rpl29	CAAGTCCAAGAACCACACCAC
	GCAAAGCGCATGTTCCCTCAG
aPKC- $\lambda$	TGAGCAGCCATTCACCATGA
	GGGAACACGTGGATCAGGAG
aPKC- $\zeta$	GTCAGGGCAGGGACGAAGT
	GGCGGTAGATGGACTTGTCTTCT
PKM- $\zeta$	GCTCCTTAAAGGGACGGAAGAT
	GGCTCCACGGCGGTAGA

**Table 5: AAV2 Viral Constructs.** Virus Titer of AAV2 viral constructs in infectious units/ml.

AAV2 Viral Constructs	Viral Titer (IU/ml)
pAAV-CAG-gCOMET-U6-shRNA PKMz	6.20E+12
pAAV-CAG-gCOMET-3xFlag-aPKCi	2.40E+12
pAAV-CAG-gCOMET	2.34E+12

## REFERENCES

1. Tuszynski, M.H. and O. Steward, *Concepts and methods for the study of axonal regeneration in the CNS*. Neuron, 2012. **74**(5): p. 777-91.
2. Center, N.S.C.I.S., *Facts and Figures at a Glance*. 2014: Birmingham, AL: University of Alabama at Birmingham.
3. (NEI), N.E.I. *Facts About Glaucoma*. 4/26/2015]; Available from: [https://www.nei.nih.gov/health/glaucoma/glaucoma\\_facts](https://www.nei.nih.gov/health/glaucoma/glaucoma_facts).
4. (NEI), N.E.I. *Glaucoma, Open-angle*. 2010 4/26/2015]; Available from: <https://www.nei.nih.gov/eyedata/glaucoma>.
5. (MSMR), M.S.M.R., *Eye injuries, active component, U.S. Armed Forces, 2000-2010*. 2011 May, Armed Forces Health and Surveillance Center. p. 2-7.
6. Chau, W.K., K.F. So, D. Tay, and P. Dockery, *A morphometric study of optic axons regenerated in a sciatic nerve graft of adult rats*. Restor Neurol Neurosci, 2000. **16**(2): p. 105-116.
7. David, S. and A.J. Aguayo, *Axonal elongation into peripheral nervous system "bridges" after central nervous system injury in adult rats*. Science, 1981. **214**(4523): p. 931-3.
8. Mar, F.M., T.F. da Silva, M.M. Morgado, L.G. Rodrigues, D. Rodrigues, M.I. Pereira, A. Marques, V.F. Sousa, J. Coentro, C. Sa-Miranda, M.M. Sousa, and P. Brites, *Myelin Lipids Inhibit Axon Regeneration Following Spinal Cord Injury: a Novel Perspective for Therapy*. Mol Neurobiol, 2015.
9. Geoffroy, C.G. and B. Zheng, *Myelin-associated inhibitors in axonal growth after CNS injury*. Curr Opin Neurobiol, 2014. **27**: p. 31-8.
10. Cregg, J.M., M.A. DePaul, A.R. Filous, B.T. Lang, A. Tran, and J. Silver, *Functional regeneration beyond the glial scar*. Exp Neurol, 2014. **253**: p. 197-207.

11. Bisby, M.A. and W. Tetzlaff, *Changes in cytoskeletal protein synthesis following axon injury and during axon regeneration*. Mol Neurobiol, 1992. **6**(2-3): p. 107-23.
12. Mar, F.M., A. Bonni, and M.M. Sousa, *Cell intrinsic control of axon regeneration*. EMBO Rep, 2014. **15**(3): p. 254-63.
13. Bolsover, S., J. Fabes, and P.N. Anderson, *Axonal guidance molecules and the failure of axonal regeneration in the adult mammalian spinal cord*. Restor Neurol Neurosci, 2008. **26**(2-3): p. 117-30.
14. Giger, R.J., E.R. Hollis, 2nd, and M.H. Tuszynski, *Guidance molecules in axon regeneration*. Cold Spring Harb Perspect Biol, 2010. **2**(7): p. a001867.
15. Anand, P., G. Terenghi, R. Birch, A. Wellmer, J.M. Cedarbaum, R.M. Lindsay, R.E. Williams-Chestnut, and D.V. Sinicropi, *Endogenous NGF and CNTF levels in human peripheral nerve injury*. Neuroreport, 1997. **8**(8): p. 1935-8.
16. Boyd, J.G. and T. Gordon, *Glial cell line-derived neurotrophic factor and brain-derived neurotrophic factor sustain the axonal regeneration of chronically axotomized motoneurons in vivo*. Exp Neurol, 2003. **183**(2): p. 610-9.
17. Boyd, J.G. and T. Gordon, *Neurotrophic factors and their receptors in axonal regeneration and functional recovery after peripheral nerve injury*. Mol Neurobiol, 2003. **27**(3): p. 277-324.
18. Bregman, B.S., M. McAtee, H.N. Dai, and P.L. Kuhn, *Neurotrophic factors increase axonal growth after spinal cord injury and transplantation in the adult rat*. Exp Neurol, 1997. **148**(2): p. 475-94.
19. Lu, P., Y. Wang, L. Graham, K. McHale, M. Gao, D. Wu, J. Brock, A. Blesch, E.S. Rosenzweig, L.A. Havton, B. Zheng, J.M. Conner, M. Marsala, and M.H. Tuszynski, *Long-distance growth and connectivity of neural stem cells after severe spinal cord injury*. Cell, 2012. **150**(6): p. 1264-73.
20. Park, K.K., K. Liu, Y. Hu, P.D. Smith, C. Wang, B. Cai, B. Xu, L. Connolly, I. Kramvis, M. Sahin, and Z. He, *Promoting axon regeneration in the adult CNS by modulation of the PTEN/mTOR pathway*. Science, 2008. **322**(5903): p. 963-6.

21. Low, K., A. Blesch, J. Herrmann, and M.H. Tuszynski, *A dual promoter lentiviral vector for the in vivo evaluation of gene therapeutic approaches to axon regeneration after spinal cord injury*. *Gene Ther*, 2010. **17**(5): p. 577-91.
22. Do, J.T. and H.R. Scholer, *Nuclei of embryonic stem cells reprogram somatic cells*. *Stem Cells*, 2004. **22**(6): p. 941-9.
23. Takahashi, K. and S. Yamanaka, *Induction of pluripotent stem cells from mouse embryonic and adult fibroblast cultures by defined factors*. *Cell*, 2006. **126**(4): p. 663-76.
24. Seiffers, R., C.D. Mills, and C.J. Woolf, *ATF3 increases the intrinsic growth state of DRG neurons to enhance peripheral nerve regeneration*. *J Neurosci*, 2007. **27**(30): p. 7911-20.
25. Raivich, G., M. Bohatschek, C. Da Costa, O. Iwata, M. Galiano, M. Hristova, A.S. Nateri, M. Makwana, L. Riera-Sans, D.P. Wolfer, H.P. Lipp, A. Aguzzi, E.F. Wagner, and A. Behrens, *The AP-1 transcription factor c-Jun is required for efficient axonal regeneration*. *Neuron*, 2004. **43**(1): p. 57-67.
26. Cotta-Grand, N., C. Rovere, A. Guyon, A. Cervantes, F. Brau, and J.L. Nahon, *Melanin-concentrating hormone induces neurite outgrowth in human neuroblastoma SH-SY5Y cells through p53 and MAPKinase signaling pathways*. *Peptides*, 2009. **30**(11): p. 2014-24.
27. Jankowski, M.P., S.L. McIlwrath, X. Jing, P.K. Cornuet, K.M. Salerno, H.R. Koerber, and K.M. Albers, *Sox11 transcription factor modulates peripheral nerve regeneration in adult mice*. *Brain Res*, 2009. **1256**: p. 43-54.
28. Schwaiger, F.W., G. Hager, A.B. Schmitt, A. Horvat, G. Hager, R. Streif, C. Spitzer, S. Gamal, S. Breuer, G.A. Brook, W. Nacimiento, and G.W. Kreutzberg, *Peripheral but not central axotomy induces changes in Janus kinases (JAK) and signal transducers and activators of transcription (STAT)*. *Eur J Neurosci*, 2000. **12**(4): p. 1165-76.
29. Tedeschi, A., T. Nguyen, R. Puttagunta, P. Gaub, and S. Di Giovanni, *A p53-CBP/p300 transcription module is required for GAP-43 expression, axon outgrowth, and regeneration*. *Cell Death Differ*, 2009. **16**(4): p. 543-54.

30. Kaufmann, L.T., M.S. Gierl, and C. Niehrs, *Gadd45a, Gadd45b and Gadd45g expression during mouse embryonic development*. *Gene Expr Patterns*, 2011. **11**(8): p. 465-70.
31. Sun, Y., T. Fei, T. Yang, F. Zhang, Y.G. Chen, H. Li, and Z. Xu, *The suppression of CRMP2 expression by bone morphogenetic protein (BMP)-SMAD gradient signaling controls multiple stages of neuronal development*. *J Biol Chem*, 2010. **285**(50): p. 39039-50.
32. Kulcenty, K., J. Wroblewska, S. Mazurek, E. Liszewska, and J. Jaworski, *Molecular mechanisms of induced pluripotency*. *Contemp Oncol (Pozn)*, 2015. **19**(1a): p. A22-9.
33. Whittle, C.M., E. Lazakovitch, R.M. Gronostajski, and J.D. Lieb, *DNA-binding specificity and in vivo targets of Caenorhabditis elegans nuclear factor I*. *Proc Natl Acad Sci U S A*, 2009. **106**(29): p. 12049-54.
34. Wang, S.M., Y.C. Lee, C.Y. Ko, M.D. Lai, D.Y. Lin, P.C. Pao, J.Y. Chi, Y.W. Hsiao, T.L. Liu, and J.M. Wang, *Increase of zinc finger protein 179 in response to CCAAT/enhancer binding protein delta conferring an antiapoptotic effect in astrocytes of Alzheimer's disease*. *Mol Neurobiol*, 2015. **51**(1): p. 370-82.
35. Bahr, M. and C. Przyrembel, *Myelin from peripheral and central nervous system is a nonpermissive substrate for retinal ganglion cell axons*. *Exp Neurol*, 1995. **134**(1): p. 87-93.
36. Tiscornia, G., O. Singer, and I.M. Verma, *Production and purification of lentiviral vectors*. *Nat Protoc*, 2006. **1**(1): p. 241-5.
37. McCall, J., L. Nicholson, N. Weidner, and A. Blesch, *Optimization of adult sensory neuron electroporation to study mechanisms of neurite growth*. *Front Mol Neurosci*, 2012. **5**: p. 11.
38. Ciani, L. and P.C. Salinas, *WNTs in the vertebrate nervous system: from patterning to neuronal connectivity*. *Nat Rev Neurosci*, 2005. **6**(5): p. 351-62.

39. Fernandez-Martos, C.M., C. Gonzalez-Fernandez, P. Gonzalez, A. Maqueda, E. Arenas, and F.J. Rodriguez, *Differential expression of Wnts after spinal cord contusion injury in adult rats*. PLoS One, 2011. **6**(11): p. e27000.
40. Clevers, H., K.M. Loh, and R. Nusse, *Stem cell signaling. An integral program for tissue renewal and regeneration: Wnt signaling and stem cell control*. Science, 2014. **346**(6205): p. 1248012.
41. Sacktor, T.C., *Memory maintenance by PKMzeta--an evolutionary perspective*. Mol Brain, 2012. **5**: p. 31.
42. Wu-Zhang, A.X., C.L. Schramm, S. Nabavi, R. Malinow, and A.C. Newton, *Cellular pharmacology of protein kinase Mzeta (PKMzeta) contrasts with its in vitro profile: implications for PKMzeta as a mediator of memory*. J Biol Chem, 2012. **287**(16): p. 12879-85.
43. Lee, A.M., B.R. Kanter, D. Wang, J.P. Lim, M.E. Zou, C. Qiu, T. McMahon, J. Dadgar, S.C. Fischbach-Weiss, and R.O. Messing, *Prkcz null mice show normal learning and memory*. Nature, 2013. **493**(7432): p. 416-9.
44. Parker, S.S., E.K. Mandell, S.M. Hapak, I.Y. Maskaykina, Y. Kusne, J.Y. Kim, J.K. Moy, P.A. St John, J.M. Wilson, K.M. Gothard, T.J. Price, and S. Ghosh, *Competing molecular interactions of aPKC isoforms regulate neuronal polarity*. Proc Natl Acad Sci U S A, 2013. **110**(35): p. 14450-5.
45. Shi, S.H., L.Y. Jan, and Y.N. Jan, *Hippocampal neuronal polarity specified by spatially localized mPar3/mPar6 and PI 3-kinase activity*. Cell, 2003. **112**(1): p. 63-75.
46. Minis, A., D. Dahary, O. Manor, D. Leshkowitz, Y. Pilpel, and A. Yaron, *Subcellular transcriptomics-dissection of the mRNA composition in the axonal compartment of sensory neurons*. Dev Neurobiol, 2014. **74**(3): p. 365-81.
47. Sarbassov, D.D., D.A. Guertin, S.M. Ali, and D.M. Sabatini, *Phosphorylation and regulation of Akt/PKB by the rictor-mTOR complex*. Science, 2005. **307**(5712): p. 1098-101.

48. Baldwin, K.T., K.S. Carbajal, B.M. Segal, and R.J. Giger, *Neuroinflammation triggered by beta-glucan/dectin-1 signaling enables CNS axon regeneration*. Proc Natl Acad Sci U S A, 2015. **112**(8): p. 2581-6.
49. Benowitz, L.I. and Y. Yin, *Optic nerve regeneration*. Arch Ophthalmol, 2010. **128**(8): p. 1059-64.
50. Yin, Y., Q. Cui, Y. Li, N. Irwin, D. Fischer, A.R. Harvey, and L.I. Benowitz, *Macrophage-derived factors stimulate optic nerve regeneration*. J Neurosci, 2003. **23**(6): p. 2284-93.
51. Faurschou, A. and R. Gniadecki, *TNF-alpha stimulates Akt by a distinct aPKC-dependent pathway in premalignant keratinocytes*. Exp Dermatol, 2008. **17**(12): p. 992-7.
52. Hussain, A.R., S.O. Ahmed, M. Ahmed, O.S. Khan, S. Al Abdulmohsen, L.C. Plataniias, K.S. Al-Kuraya, and S. Uddin, *Cross-talk between NFkB and the PI3-kinase/AKT pathway can be targeted in primary effusion lymphoma (PEL) cell lines for efficient apoptosis*. PLoS One, 2012. **7**(6): p. e39945.
53. Leon, S., Y. Yin, J. Nguyen, N. Irwin, and L.I. Benowitz, *Lens injury stimulates axon regeneration in the mature rat optic nerve*. J Neurosci, 2000. **20**(12): p. 4615-26.
54. Wooten, M.W., *Function for NF-kB in neuronal survival: regulation by atypical protein kinase C*. J Neurosci Res, 1999. **58**(5): p. 607-11.
55. Moscat, J., P. Rennert, and M.T. Diaz-Meco, *PKCzeta at the crossroad of NF-kappaB and Jak1/Stat6 signaling pathways*. Cell Death Differ, 2006. **13**(5): p. 702-11.